

# Inverse Power Flow Problem

Ye Yuan, *Senior Member, IEEE*, Steven H. Low, *Fellow, IEEE*,  
Omid Ardakanian, *Member, IEEE*, Claire J. Tomlin, *Fellow, IEEE*

**Abstract**—This paper formulates an inverse power flow problem which is to infer a nodal admittance matrix (hence the network structure of a power system) from voltage and current phasors measured at a number of buses. We show that the admittance matrix can be uniquely identified from a sequence of measurements corresponding to different steady states when every node in the system is equipped with a measurement device, and a Kron-reduced admittance matrix can be determined even if some nodes in the system are not monitored (hidden nodes). Furthermore, we propose effective algorithms based on graph theory to uncover the actual admittance matrix of radial systems with hidden nodes. We provide theoretical guarantees for the recovered admittance matrix and demonstrate that the actual admittance matrix can be fully recovered even from the Kron-reduced admittance matrix under some mild assumptions. Simulations on standard test systems confirm that these algorithms are capable of providing accurate estimates of the admittance matrix from noisy sensor data.

**Index Terms**—Inverse Power Flow Problem, System Identification, Kron Reduction, Phasor Measurement Units.

## I. INTRODUCTION

THE power industry has witnessed profound changes in recent years. These changes are mostly driven by the widespread adoption of distributed energy resources (DER), active participation of customers in emerging energy markets, and rapid deployment of measurement, communication, and control infrastructure resulting in an unprecedented level of visibility and controllability, especially for distribution grids. Despite the increased amount of uncertainty, these changes offer opportunities for system operators to improve power system stability and efficiency by leveraging advanced optimization and control techniques. Most of these techniques require the knowledge of the network topology in real time.

The inverse power flow (IPF) problem we define in this paper concerns the estimation of the nodal admittance matrix from synchronized measurements of voltage and current phasors (i.e., magnitudes and phase angles) which can be obtained from phasor measurement units (PMUs) or conventional supervisory control and data acquisition (SCADA) technology. The IPF problem underlies several crucial smart grid applications, affecting real-time system operation and long-term planning, the most important of which are:

1) *State Estimation* [1] combines the knowledge of the admittance matrix with a set of known state-variables to determine the unknown ones, e.g., voltage magnitude and phase angle of unobserved buses, thereby building a real-time model of the network for control.

2) *Optimization & Control* [2] techniques determine a sequence of operations that can transition the power system from one steady state to another steady state that meets certain stability and efficiency targets.

3) *Event Detection* [3] concerns identifying faults, line outages, and other critical events, such as transformer tap changes, capacitor and switching operations from changes in the real-time network model.

4) *Cybersecurity* [4] is the problem of identifying the potential vulnerabilities of a power system and designing strategies to protect it from the potential cyber attacks using telemetry data along with information about its topology.

In this paper, we lay out a theoretical framework for the IPF problem. Using the bus injection model (BIM), we propose efficient algorithms to identify the admittance matrix. In particular, we show that when the system has no hidden nodes, the admittance matrix can be uniquely identified from a sequence of complex voltage and current measurements corresponding to different steady states. Should there be some hidden nodes in the network, we show that a reduced admittance matrix (from Kron reduction [5]) can be determined; we develop a method based on graph decomposition, maximal clique searching and composition for identifying the admittance matrix of the original system for radial networks. Power flow simulations are performed on the IEEE 14-bus system to illustrate the theoretical results and evaluate their sensitivity to measurement noise introduced by transducers.

The paper is outlined as follows: after surveying related work in Section II, we formulate the IPF problem and propose a solution for the case that the system is fully observable in Section III. When the system has hidden nodes, we propose efficient algorithms to solve the IPF problem for radial networks with theoretical guarantee in Section IV. We evaluate the identification accuracy of the proposed algorithms in Section V and conclude the paper by presenting directions for future work in Section VI.

## II. RELATED WORK

The availability of high-precision, high-sample-rate measurements of transmission and distribution networks in recent years has given impetus to research on topology and admittance identification.

The IPF problem that identifies both topology and admittance matrix has been studied extensively in transmission

Ye Yuan is with School of Artificial Intelligence and Automation, Huazhong University of Science and Technology, Wuhan, China. Steven H. Low is with Department of Computer and Mathematical Sciences and Electrical Engineering, California Institute of Technology, Pasadena, United States. Omid Ardakanian is with Department of Computing Science, University of Alberta, Edmonton, Canada. Claire J. Tomlin is with Department of Electrical Engineering and Computer Sciences, University of California, Berkeley, United States. Correspondence to slow@caltech.edu.

This version corrects the proof to Proposition 3 and adds details about constructing the admittance matrix of the overall network from its components.

networks [6], [7], [8], [9] as well as distribution grids [10], [11] using single-phase a.c. and d.c. power flow models. For example, the topology identification problem is cast as a sparse subspace learning problem in [6] and an efficient algorithm is proposed to estimate the admittance matrix of the underlying power system from the measured power injection of different buses. In [12], the topology of an urban (mesh) distribution network is inferred from voltage magnitude, and real/reactive power measurements carried out by smart meters at the end-nodes. A graphical model is built to describe the probabilistic relationships between different voltage measurements using lasso. In [10] a graphical learning based approach is developed to estimate the radial grid topology from nodal voltage measurements. The learning algorithm is based on conditional independence tests for continuous variables over chordal graphs. An efficient algorithm for topology identification of a power system is also proposed in [8] drawing on ideas from compressive sensing and graph theory. The authors assume that power and phase angle measurements are available for all nodes.

Different algorithms have been developed in the literature to make this inference, using various techniques such as weighted least square, maximum-likelihood/maximum-a-posteriori estimation, minimum spanning tree, sparse recovery, Lasso/Group Lasso, blind identification, quickest change detection theory, as well as graphical model learning. There are three limitations in the current literature that we propose overcome. First, most of the literature focuses on topology identification or change detection, but there is not much work on joint topology and parameter identification, with notable exceptions of [6], [13], [14]. Second, most papers require measurements at every node in the network, with the exceptions of [15], [14], [16], [17], [18], [19]. In particular, [14] learns the topology with parameters from a stochastic perspective, the true topology can only be found in probability, even when the number of samples is large; [17], [18] assume that perturbed data are available (therefore a special inverter is assumed) to identify the network, which could be strong in practice; [19] proposed a method based on recursive grouping to estimate the topology and branch impedance for networks that may have hidden nodes, however, without guarantee.

### III. IPF WITHOUT HIDDEN NODES

In this section we study the IPF problem when voltage and current phasor measurements are available at every bus in the system. We formulate the identification problem as a constrained least squares problem and then convert it to an equivalent unconstrained least squares problem. We note that  $Y$  has a certain structure that can be exploited when solving the IPF problem— (a)  $Y$  is a symmetric but not Hermitian complex matrix (i.e.,  $Y \in \mathbb{S}^N$ ) and (b)  $Y$  encodes the topology of a connected graph (or a connected tree for radial networks).

#### A. Problem formulation

Let  $\mathbb{C}$  denote the set of complex numbers,  $\mathbb{R}$  the set of real numbers, and  $\mathbb{N}$  the set of integers. For  $A \in \mathbb{C}^{n \times n}$ ,  $\text{Re}(A)$  and  $\text{Im}(A)$  denote matrices with the real and imaginary parts

of  $A$ , respectively. Let  $\mathbb{S}^n \subseteq \mathbb{C}^{n \times n}$  be the set of all  $n \times n$  complex symmetric (not necessarily Hermitian) matrices. The transpose of a matrix  $A$  is denoted  $A^T$  and its Hermitian (complex conjugate) transpose is denoted  $A^H$ .  $A[i, j]$  denotes the element of  $A$  located at  $i$ th row and  $j$ th column. We define  $\mathcal{I}$  as the identity matrix with an appropriate dimension and define  $\mathbf{1}$  as an all-1 column vector with an appropriate dimension.

A power system can be modeled by an undirected connected graph  $\mathcal{G} = (\mathcal{N}, \mathcal{E})$  where  $\mathcal{N} := \{1, 2, \dots, N\}$  represents the set of buses, and  $\mathcal{E} \subseteq \mathcal{N} \times \mathcal{N}$  represents the set of lines, each connecting two distinct buses. A bus  $j \in \mathcal{N}$  can be a load bus, a generator bus, or a swing bus. Let  $V_j$  be the complex voltage at bus  $j$  and  $s_j$  be the net complex power injection (generation minus load) at that bus. We use  $s_j$  to denote both the complex number  $p_j + \mathbf{i}q_j$  ( $\mathbf{i} \triangleq \sqrt{-1}$ ) and the real pair  $(p_j, q_j)$  depending on the context. For each line  $(i, j) \in \mathcal{E}$ , we denote its series admittance by  $y_{ij}$ . The bus admittance matrix of this system is denoted  $Y$ , which is an  $N \times N$  complex-valued matrix whose off-diagonal elements are  $Y_{ij} = -y_{ij}$  and diagonal elements are  $Y_{ii} = -\sum_{j \neq i} Y_{ij}$ , assuming that there is no shunt element (this assumption can be relaxed). Hence, the current injection vector can be expressed as  $I = YV$ .

The formulated IPF problem is: given voltage and current measurements of different steady-states, i.e.,  $V_i(k)$  and  $I_i(k)$  for  $k = 1, \dots, K$  and  $i \in \mathcal{M} = \{1, \dots, N\}$ , how to recover the true admittance matrix  $Y$ . Specially, when  $\mathcal{M}$  is a subset of  $\mathcal{N}$ , what part of the true admittance matrix  $Y$  can be recovered under what condition.

#### B. Identification algorithm

In this section, we consider the case when  $\mathcal{M} = \{1, \dots, N\}$  and propose a solution to the IPF. We will relax this full measurement condition, i.e., when  $\mathcal{M} \subset \{1, \dots, N\}$  in the next section.

For  $k \in \{1, \dots, K\}$ , the Kirchhoff's laws for a given time index yields  $I(k) = YV(k)$ . Rewriting this formula in vector form for all time indices yields the following equation for a bus  $i$ :

$$\underbrace{\begin{bmatrix} I_i(1) \\ I_i(2) \\ \vdots \\ I_i(K) \end{bmatrix}}_{I_i^K} = \underbrace{\begin{bmatrix} V_1(1) & V_2(1) & \dots & V_N(1) \\ V_1(2) & V_2(2) & \dots & V_N(2) \\ \vdots & \vdots & \ddots & \vdots \\ V_1(K) & V_2(K) & \dots & V_N(K) \end{bmatrix}}_{V^K} \underbrace{\begin{bmatrix} Y_{i1} \\ Y_{i2} \\ \vdots \\ Y_{iN} \end{bmatrix}}_{Y_i}. \quad (1)$$

The admittance matrix  $Y$  can be obtained from solving the optimization problem below:

$$\hat{Y}^{K, l_2} \triangleq \arg \min_Y \|V^K Y - I^K\|_F \quad (2)$$

s.t.:  $Y \in \mathbb{S}^N$ ,  $Y_{ii} = -\sum_{j \neq i} Y_{ij}$ ,  $\forall i$ .

in which  $I^K$  is a  $K \times N$  matrix, i.e.,  $I^K = \begin{bmatrix} I_1^K & I_2^K & \dots & I_N^K \end{bmatrix}$ . Define

$$\text{vec}(Y) = [Y_{11} \ Y_{21} \ \dots \ Y_{N1} \ Y_{12} \ Y_{22} \ \dots \ Y_{NN}]^T,$$

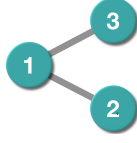


Fig. 1. An illustrative example of a three-node power system with two lines connecting bus 1 to buses 2 and 3 respectively.

and apply the  $\text{vec}$  operator to the objective function, we obtain:

$$\begin{aligned} \min_{\text{vec}(Y) \in \mathbb{C}^{N^2 \times 1}} & \left\| (\mathcal{I} \otimes V^K) \text{vec}(Y) - \text{vec}(I^K) \right\|_2 \quad (3) \\ \text{s.t.}: & Y \in \mathbb{S}^N, \quad Y_{ii} = -\sum_{j \neq i} Y_{ij}, \quad \forall i, \end{aligned}$$

where  $\otimes$  is the Kronecker product. This holds because  $\text{vec}(ABC) = (C^T \otimes A)\text{vec}(B)$ . Let  $\text{svec} : \mathbb{S}^N \rightarrow \mathbb{C}^{(N^2-N)/2 \times 1}$  be a mapping from a symmetric complex matrix to a complex vector defined as:

$$\text{svec}(Y) = [Y_{21} \quad Y_{31} \quad \dots \quad Y_{N1} \quad Y_{32} \quad Y_{42} \quad \dots \quad Y_{NN-1}]^T.$$

It can be readily seen that  $\text{svec}$  is a bijection for any matrix  $Y$  that satisfies a)  $Y \in \mathbb{S}^N$  and b)  $1^T Y = 0$ . Based on this definition, we have  $\text{vec}(Y) = \Gamma \text{svec}(Y)$ , where  $\Gamma \in \mathbb{R}^{N^2 \times (N^2-N)/2}$  maps  $\text{svec}(Y)$  to the vectorized admittance matrix as illustrated below.

**Example 1.** For the network depicted in Figure 1, the  $\Gamma$  matrix has the following form

$$\underbrace{\begin{bmatrix} Y_{11} \\ Y_{21} \\ Y_{31} \\ Y_{12} \\ Y_{22} \\ Y_{32} \\ Y_{13} \\ Y_{23} \\ Y_{33} \end{bmatrix}}_{\text{vec}(Y)} = \underbrace{\begin{bmatrix} -1 & -1 & 0 \\ 1 & 0 & 0 \\ 0 & 1 & 0 \\ 1 & 0 & 0 \\ -1 & 0 & -1 \\ 0 & 0 & 1 \\ 0 & 1 & 0 \\ 0 & 0 & 1 \\ 0 & -1 & -1 \end{bmatrix}}_{\Gamma} \underbrace{\begin{bmatrix} Y_{21} \\ Y_{31} \\ Y_{32} \end{bmatrix}}_{\text{svec}(Y)}.$$

Based on the definition of  $\Gamma$  in the above equation, the constrained optimization problem can be converted to an unconstrained one:

$$\min_{\text{svec}(Y) \in \mathbb{C}^{(N^2-N)/2 \times 1}} \left\| \underbrace{(\mathcal{I} \otimes V^K)}_F \Gamma \text{svec}(Y) - \text{vec}(I^K) \right\|_2, \quad (4)$$

in which  $\mathcal{I}$  denotes an identity matrix and  $F \triangleq (\mathcal{I} \otimes V^K)\Gamma$ . We define

$$\tilde{F} = \begin{bmatrix} \text{Re}(F) & -\text{Im}(F) \\ \text{Im}(F) & \text{Re}(F) \end{bmatrix}, \quad \text{and} \quad \tilde{b} = \begin{bmatrix} \text{Re}(\text{vec}(I^K)) \\ \text{Im}(\text{vec}(I^K)) \end{bmatrix}.$$

The optimization problem (4) can be written as an unconstrained quadratic program in the real domain:

$$\min_{\tilde{f}(Y) \in \mathbb{R}^{(N^2-N) \times 1}} \left\| \tilde{F} \tilde{f}(Y) - \tilde{b} \right\|_2, \quad (5)$$

in which  $\tilde{f}(Y) \triangleq [\text{svec}(Y_R)^T \quad \text{svec}(Y_I)^T]^T$ ,  $Y_R = \text{Re}(Y)$ , and  $Y_I = \text{Im}(Y)$ . This least square problem yields a solution

provided that  $\tilde{M}$  has full column rank:

$$\tilde{f}(Y) = \left( \tilde{F}^T \tilde{F} \right)^{-1} \tilde{F}^T \tilde{b}. \quad (6)$$

We compute the solution of the original optimization problem (4) from the solution of the optimization problem (5) by taking the inverse map of  $\tilde{f}$ . A sufficient condition to guarantee the exactness of the solution is that  $V^K$  has full column rank. When  $V^K$  does not have full column rank, we can characterize the part of the admittance matrix that is identifiable (see [3]).

**Proposition 1 (Exactness).** *If  $V^K$  has full column rank, the optimization problem (5) has a unique solution given by (6).*

*Proof:* Since  $\Gamma \in \mathbb{R}^{N^2 \times (N^2-N)/2}$  and has full column rank (this can be checked easily), there exists a matrix  $\Gamma^\dagger$  such that  $\Gamma^\dagger \Gamma = \mathcal{I}$ . For the Kronecker product  $\mathcal{I} \otimes V^K \in \mathbb{C}^{KN \times N^2}$ ,  $\mathcal{I} \otimes V^K$  has full column rank when  $V^K$  has full column rank; therefore,  $\tilde{F}$  and  $F$  have full column rank given the fact that  $\text{rank}(\tilde{F}) = 2\text{rank}(F)$ .

Finally, we prove by contradiction that if  $\tilde{F}$  has full column rank, the solution to the optimization problem (5) is unique. Suppose there exists  $\tilde{f}(Y_1)$  and  $\tilde{f}(Y_2)$  ( $\tilde{f}(Y_1) \neq \tilde{f}(Y_2)$ ) such that  $\tilde{F} \tilde{f}(Y_1) = \tilde{b}$  and  $\tilde{F} \tilde{f}(Y_2) = \tilde{b}$ , then

$$\tilde{F} \left( \tilde{f}(Y_1) - \tilde{f}(Y_2) \right) = 0,$$

which contradicts the full column rank assumption. ■

**Remark 1.** The approach can be easily extended to the case of nonzero shunt elements where  $1^T Y \neq 0$  by changing the definitions of  $\text{svec}(Y)$ ,  $\Gamma$  and  $\tilde{f}(\cdot)$ . Specifically if  $Y$  includes shunt elements then  $\text{svec}(Y)$  will include diagonal elements ( $Y_{11}, \dots, Y_{NN}$ ).

We can add the element-wise positivity constraint to this problem if the conductance and susceptance of each line are positive<sup>1</sup>.

$$\min_{\tilde{f}(Y) \geq 0} \left\| \tilde{F} \tilde{f}(Y) - \tilde{b} \right\|_2. \quad (7)$$

The above problem is known as nonnegative least squares, which is a convex optimization problem and a global minimizer can be solved using different methods, such as the active set method [20].

#### IV. IPF WITH HIDDEN NODES

In the previous section we solve the IPF problem when voltage and current measurements are available at all buses. In this section we consider the case when voltage and current measurements are available only at a subset of the buses. In a distribution system, for example, measurements are typically available at the substation and customer meters but not throughout the grid.

In Section IV-A, we show that, in the presence of hidden nodes, the algorithm presented in Section III can identify a Kron-reduced admittance matrix  $\tilde{Y}$ , defined in (11) below, for the nodes where measurements are available (Corollary 1). In Section IV-B we show that when the network is a tree

<sup>1</sup>The conductance of a line is always positive, the susceptance can be negative or positive depending on whether the line is inductive or capacitive.

then it is indeed possible to uniquely identify the original admittance matrix  $Y$  from its Kron reduction under reasonable assumptions.

### A. Kron-reduced admittance matrix $\bar{Y}$

We call a bus/node a *measured bus/node* if measurements of its voltage and current injection are available for identification. We call it a *hidden bus/node* otherwise. Let  $\mathcal{M}$  and  $\mathcal{H}$  represent the set of measured and hidden nodes respectively.

**Assumption 1.** We make the following assumptions:

- 1.1 The underlying graph  $\mathcal{G}$  is connected.
- 1.2 Hidden nodes have zero injection  $I_i(k) = 0$  for all  $i \in \mathcal{H}$ .

Note that the second assumption, i.e., the injected current is zero at every hidden node, is reasonable because if generators or loads are connected to a node, then the current they inject or draw is typically measured.

Let  $H$  be the number of hidden nodes. Without loss of generality we label the buses so that the first  $N - H$  buses are measured and the last  $H$  buses are hidden, i.e.,  $\mathcal{M} := \{1, \dots, M \triangleq N - H\}$  and  $\mathcal{H} := \{N - H + 1, \dots, N\}$ . We partition the bus admittance matrix  $Y$  into four sub-matrices:

$$\begin{aligned} Y &= \begin{bmatrix} Y_{11} & Y_{12} \\ Y_{21} & Y_{22} \end{bmatrix} = \begin{bmatrix} G_{11} & G_{12} \\ G_{21} & G_{22} \end{bmatrix} + \mathbf{i} \begin{bmatrix} B_{11} & B_{12} \\ B_{21} & B_{22} \end{bmatrix} \\ &= G + \mathbf{i}B. \end{aligned} \quad (8)$$

Here  $Y_{11} \in \mathbb{S}^{N-H}$  describes the connectivity among the measured nodes,  $Y_{12} = Y_{21}^T \in \mathbb{C}^{(N-H) \times H}$  the connectivity between the measured and the hidden nodes, and  $Y_{22} \in \mathbb{S}^H$  the connectivity among the hidden nodes. For  $i \in \mathcal{M}$ ,  $(I_i(k), V_i(k), k = 1, \dots, K)$  denote the current and voltage measurements at bus  $i$  at time  $k$ . To simplify notation, we index the entries of  $Y_{22}$ , not by  $i, j = 1, \dots, H$ , but by  $i, j = N - H + 1, \dots, N$ . We index the entries of  $Y_{12}$  by  $i = 1, \dots, N - H$  and  $j = N - H + 1, \dots, N$  and similarly for  $Y_{21} = Y_{12}^T$ , as well as submatrices  $G_{ij}, B_{ij}$  in (8).

For  $i \in \mathcal{H}$ ,  $I_i(k) = 0$ ,  $\forall k$ , and  $V_i(k)$  is the voltage at bus  $i$  but is not available for identification. To simplify notation, We abuse  $V_1(k)$  to denote both the voltage at bus 1 at time  $k$  and the vector of all voltages at measured buses at time  $k$ , depending on the context; similarly for  $V_2(k)$  and  $I_1(k)$ . Then

$$\begin{bmatrix} I_1(k) \\ 0 \end{bmatrix} = \begin{bmatrix} Y_{11} & Y_{12} \\ Y_{21} & Y_{22} \end{bmatrix} \begin{bmatrix} V_1(k) \\ V_2(k) \end{bmatrix}, \quad \forall k \quad (9)$$

If  $Y_{22}$  is invertible then eliminating  $V_2$  from (9) yields a relation

$$I_1(k) = \bar{Y}V_1(k), \quad \forall k \quad (10)$$

between currents and voltages at measured nodes through the *Kron-reduced admittance matrix*  $\bar{Y} \in \mathbb{S}^m$  defined as:

$$\bar{Y} \triangleq Y_{11} - Y_{12}Y_{22}^{-1}Y_{12}^T \quad (11)$$

for the set of measured nodes. In the rest of this subsection we first justify the invertibility of  $Y_{22}$  and hence the definition of  $\bar{Y}$ . Proposition 1 then implies that  $\bar{Y}$  can be identified from voltage and current measurements. Moreover  $\bar{Y}$  is the best we

can identify for general networks because multiple admittance matrices  $Y$  may reduce to the same  $\bar{Y}$ .

**Assumption 2.** The admittance matrix  $Y \triangleq G + \mathbf{i}B$  defined in (8) satisfies:

- 2.1 Series impedances of the lines are resistive and inductive:  $G[i, j] \leq 0$  and  $B[i, j] \geq 0$  for any  $i \neq j$ ;
- 2.2 Diagonal dominance:  $G_{22}[i, i] \geq -\sum_{j \neq i} G_{22}[i, j]$  and  $-B_{22}[i, i] \geq \sum_{j \neq i} B_{22}[i, j]$  hold for any  $i$ .

**Lemma 1.** Under Assumption 1 and 2,  $G_{22} \succeq 0$ ,  $-B_{22} \succeq 0$  and  $G_{22} - B_{22} \succ 0$ , when  $H < N$ .

*Proof:* From the Gershgorin Theorem and Assumption 2.2, all eigenvalues of the submatrix  $G_{22}$  lie in the right-half plane including the origin and all eigenvalues of  $B_{22}$  lie in the left-half plane including the origin. Together with the fact that  $G_{22}$  and  $B_{22}$  are symmetric, we have  $G_{22} \succeq 0$  and  $-B_{22} \succeq 0$ .

This implies that  $G_{22} - B_{22} \succeq 0$ . We now show that indeed  $G_{22} - B_{22} \succ 0$ . Suppose for the sake of contradiction that there exists a nonzero  $x \in \mathbb{R}^H$  such that  $x^T(G_{22} - B_{22})x = 0$ . Denote by  $A_{22} := G_{22} - B_{22}$  and  $A_{21} := G_{21} - B_{21}$  so that

$$A_{22}[i, i] = \sum_{i, j \in \mathcal{H}: j \neq i} (-A_{22}[i, j]) + \sum_{i \in \mathcal{H}, j \in \mathcal{M}} (-A_{21}[i, j])$$

Then

$$\begin{aligned} x^T(G_{22} - B_{22})x &= \sum_{i, j \in \mathcal{H}: i \neq j} (A_{22}[i, j]x_i x_j - A_{22}[i, j]x_i^2) \\ &\quad + \sum_{i \in \mathcal{H}, j \in \mathcal{M}} (-A_{21}[i, j])x_i^2 \\ &= \sum_{i, j \in \mathcal{H}: i < j} (-A_{22}[i, j])(x_i - x_j)^2 \\ &\quad + \sum_{i \in \mathcal{H}, j \in \mathcal{M}} (-A_{21}[i, j])x_i^2 \end{aligned} \quad (12)$$

By definition  $A_{22}[i, j] = A_{21}[i, j] = 0$  if  $i \not\sim j$  (i.e.,  $i$  and  $j$  are not adjacent). For  $i, j \in \mathcal{M} \cup \mathcal{H}$ , if  $i \sim j$  (i.e.,  $i$  and  $j$  are adjacent), then  $Y_{ij} = G_{ij} + \mathbf{i}B_{ij} \neq 0$ , i.e., at least one of  $G_{ij} = -g_{ij} \leq 0$  or  $B_{ij} = -b_{ij} \geq 0$  is nonzero. This implies that  $-A_{22}[i, j] = -G_{22}[i, j] + B_{22}[i, j] > 0$  and  $-A_{21}[i, j] = -G_{21}[i, j] + B_{21}[i, j] > 0$  for all  $i \sim j$ . Therefore, for  $x^T(G_{22} - B_{22})x = 0$  in (12), we must have:

1.  $x_i = x_j$  if  $i \sim j$  is a connection between hidden nodes in  $\mathcal{H}$ ;
2.  $x_i = 0$  for any hidden node  $i \in \mathcal{H}$  connected to at least one observed node  $j \in \mathcal{M}$ .

Since the network is connected, for every hidden node  $i \in \mathcal{H}$ , there is a path that connects the hidden node to an observed node  $k \in \mathcal{M}$ . For all nodes  $j$  on this path from  $i$  to  $k$ , the above properties implies that  $x_j = 0$ . Since this is true for all hidden nodes, we have  $x = 0$ , a contradiction. Hence  $G_{22} - B_{22} \succ 0$ . ■

Recall that the network is connected and has  $N$  nodes of which  $H$  are hidden.

**Proposition 2.** Under Assumptions 1 and 2, if  $H < N$  then  $Y_{22}$  is invertible.

*Proof:* We prove that 0 is not an eigenvalue of  $Y_{22}$ . Suppose for the sake of contradiction that there exists a nonzero vector  $(v + iw)$  such that  $(G_{22} + iB_{22})(v + iw) = 0$ , i.e.,

$$G_{22}v - B_{22}w = 0 \quad \text{and} \quad G_{22}w + B_{22}v = 0,$$

This implies

$$\begin{aligned} (G_{22} + B_{22})v + (G_{22} - B_{22})w &= 0, \\ (G_{22} + B_{22})w - (G_{22} - B_{22})v &= 0. \end{aligned} \quad (13)$$

Since  $G_{22} - B_{22} \succ 0$  by Lemma 1, we can eliminate  $v$  from (13) to get

$$((G_{22} - B_{22}) + (G_{22} + B_{22})(G_{22} - B_{22})^{-1}(G_{22} + B_{22}))w = 0.$$

Multiplying  $w^T$  on the left we have

$$w^T(G_{22} - B_{22})w + \hat{w}^T(G_{22} - B_{22})^{-1}\hat{w} = 0,$$

where  $\hat{w} = (G_{22} + B_{22})w$ . This contradicts  $G_{22} - B_{22} \succ 0$  unless  $w = 0$ . But  $w = 0$  implies that  $(G_{22} - B_{22})v = 0$  from (13), meaning  $v = 0$ . This is a contradiction and hence  $Y_{22}$  is invertible. ■

Proposition 2 guarantees that  $Y_{22}$  is invertible and hence the Kron-reduced admittance  $\bar{Y}$  in (11) is well defined under Assumption 2. Moreover, because of (10), the algorithm in Section III can identify the Kron-reduced admittance matrix  $\bar{Y}$  from voltage and current measurements (Proposition 1).

**Corollary 1.** *Suppose Assumptions 1 and 2 and the condition in Proposition 1 hold. If  $H < N$ , then the Kron-reduced admittance matrix  $\bar{Y}$  can be identified from voltage  $V_1^K$  and current  $I_1^K$  measurements at the measured nodes.*

An admittance matrix  $Y \in \mathbb{S}^N$  specifies a unique weighted undirected graph  $\mathcal{G}(Y) = (\mathcal{N}(Y), \mathcal{E}(Y))$  with  $\mathcal{N} := \{1, \dots, N\}$  and  $\mathcal{E} \subseteq \mathcal{N} \times \mathcal{N}$  such that there is an edge  $(i, j)$  if and only if  $Y[i, j] \neq 0$ . Its Kron reduction  $\bar{Y}$  specifies a unique weighted graph  $\bar{\mathcal{G}} := \mathcal{G}(\bar{Y}) = (\mathcal{M}, \bar{\mathcal{E}})$  that can be obtained from  $\mathcal{G}$  through Algorithm 1.

---

#### Algorithm 1 Graph Condensation Algorithm

---

- 1: **Input:** a graph  $\mathcal{G} = (\mathcal{N}, \mathcal{E})$  with  $N$  nodes and a set of measured nodes  $\mathcal{M} = \{1, 2, \dots, M\}$  and admittance matrix  $Y$
  - 2: **for**  $v = M + 1 : N$  **do**
  - 3:   Remove hidden node  $v$  from  $\mathcal{N} = \mathcal{N} - \{v\}$  and all edges from  $\mathcal{E}$  that are incident on  $v$ ;
  - 4:   For all node pairs  $w$  and  $l$  that are neighbors of  $v$ , add an edge between  $w$  and  $l$  to  $\mathcal{E}$ ;
  - 5:   Update the admittance matrix  $Y = Y/Y[i, i]$  using eq. (15).
  - 6: **end for**
  - 7: **return**  $\bar{\mathcal{G}} = \mathcal{G}$  and  $\bar{Y} = Y$ .
- 

Each iterative step in the algorithm removes a hidden node  $i \in \mathcal{H}$  and connects all its neighbors to each other. This step can be represented algebraically as an update on the admittance matrix to compute its Schur complement of  $Y[i, i]$ . Specifically we can partition possibly after permutation an

admittance matrix  $Y$  of an appropriate dimension into the form:

$$Y = \begin{bmatrix} Y(i, i) & Y(i, i] \\ Y(i, i]^T & Y[i, i] \end{bmatrix},$$

where  $Y[i, i] \in \mathbb{C}$  is the  $i$ th diagonal elements of  $Y$ , and  $Y(i, i), Y(i, i]$  are shown in Eq. (14). Then each iterative step of Algorithm 1 updates the admittance matrix by  $(Y[i, i])^{-1}$  is always invertible due to Proposition 2):

$$Y/Y[i, i] = Y(i, i) - Y(i, i]Y^{-1}[i, i]Y(i, i]^T. \quad (15)$$

This step is repeated until all the hidden nodes are removed from the original graph, producing the Kron-reduced graph  $\bar{\mathcal{G}} = \{\mathcal{M}, \bar{\mathcal{E}}\}$  [5] and its admittance matrix  $\bar{Y}$  (shown in Fig. 2).

Given an admittance matrix  $Y$ , each partition  $(Y_{11}, Y_{12}, Y_{22})$  in (8) defines uniquely a Kron-reduced matrix  $\bar{Y} := \bar{Y}(Y_{11}, Y_{12}, Y_{22})$  given by (11). This mapping is clearly not injective in general, i.e., given an  $M \times M$  symmetric matrix  $\bar{Y} \in \mathbb{S}^M$  (possibly with  $\bar{Y}\mathbf{1} = 0$ ) there are generally multiple  $N \times N$  symmetric matrices  $Y$  that can be partitioned into (non-unique)  $(Y_{11}, Y_{12}, Y_{22})$  whose Kron reductions are the given  $\bar{Y}$ , as long as  $N \geq M$ .

**Example 2.** *Consider a (Kron-reduced) admittance matrix for a two-node network ( $\theta \neq 0$ ):*

$$\bar{Y} = \begin{bmatrix} \theta & -\theta \\ -\theta & \theta \end{bmatrix}.$$

The following  $3 \times 3$  admittance matrix  $Y$  with the given partition has  $\bar{Y}$  as its Kron reduction:

$$Y := \left[ \begin{array}{c|c} Y_{11} & Y_{12} \\ \hline Y_{12}^T & Y_{22} \end{array} \right] = \left[ \begin{array}{cc|c} \theta + \theta' & -\theta & -\theta' \\ -\theta & \theta & 0 \\ \hline -\theta' & 0 & \theta' \end{array} \right],$$

for arbitrary nonzero  $\theta'$ . The underlying network is shown in Fig. 1 with Node 3 as the hidden node, so that  $\bar{Y}$  corresponds to the Kron-reduced admittance matrix for Nodes 1 and 2 in Fig. 1. In this case the hidden node has degree 1. Another  $3 \times 3$  admittance matrices  $\tilde{Y}$  that also has  $\bar{Y}$  as its Kron reduction is:

$$\tilde{Y} := \left[ \begin{array}{c|c} \tilde{Y}_{11} & \tilde{Y}_{12} \\ \hline \tilde{Y}_{12}^T & \tilde{Y}_{22} \end{array} \right] = \left[ \begin{array}{cc|c} \theta_1 & 0 & -\theta_1 \\ 0 & \theta_2 & -\theta_2 \\ \hline -\theta_1 & -\theta_2 & \theta_1 + \theta_2 \end{array} \right],$$

as long as  $(\theta_1, \theta_2)$  satisfies

$$\frac{\theta_1\theta_2}{\theta_1 + \theta_2} = \theta.$$

The network underlying  $\tilde{Y}$  is isomorphic to that in Fig. 1 with Node 1 being the hidden node, so that  $\tilde{Y}$  is the Kron-reduced admittance matrix for Nodes 2 and 3 in Fig. 1. In this case the hidden node has degree 2.

Example 2 shows that in general only the Kron-reduced admittance matrix  $\bar{Y}$  is identifiable from measurements at the measured nodes. For arbitrary networks it is impossible to identify the original admittance matrix  $Y$  whose Kron reduction yields  $\bar{Y}$ . We next show the surprising result that, when the underlying network is a tree and every hidden nodes

$$Y(i, i) = \begin{bmatrix} Y[1, 1] & \dots & Y[1, i-1] & Y[1, i+1] & \dots & Y[1, N] \\ \vdots & \ddots & \vdots & \vdots & \ddots & \vdots \\ Y[i-1, 1] & \dots & Y[i-1, i-1] & Y[i-1, i+1] & \dots & Y[i-1, N] \\ Y[i+1, 1] & \dots & Y[i+1, i-1] & Y[i+1, i+1] & \dots & Y[i+1, N] \\ \vdots & \ddots & \vdots & \vdots & \ddots & \vdots \\ Y[N, 1] & \dots & Y[N, i-1] & Y[N, i+1] & \dots & Y[N, N] \end{bmatrix}, \quad Y(i, i) = \begin{bmatrix} Y[1, i] \\ \vdots \\ Y[i-1, i] \\ Y[i+1, i] \\ \vdots \\ Y[N, i] \end{bmatrix}. \quad (14)$$

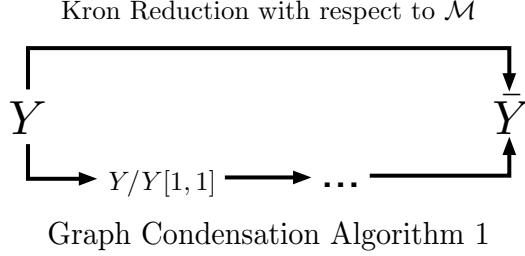


Fig. 2. Two equivalent schemes to compute the Kron reduced  $\bar{Y}$ .

has a degree  $\geq 3$ , then the original admittance matrix  $Y$  can indeed be discovered even in the presence of hidden nodes.

### B. Radial networks: exact identification

Consider a radial network and suppose we have identified a Kron-reduced admittance matrix  $\bar{Y}$  from partial voltage and current measurements. In this section we develop a novel algorithm to compute the original admittance matrix  $Y$  from  $\bar{Y}$  under the following additional assumptions.

**Assumption 3.** *The admittance matrix  $Y$  satisfies:*

- 3.1 *The underlying graph  $\mathcal{G}(Y)$  is a tree.*
- 3.2 *Every hidden node has a degree  $\geq 3$ .*
- 3.3 *There is no shunt element in  $Y$ , i.e.,  $Y\mathbf{1} = 0$ .*

**Remark 2.** *Assumption 3.2 is a necessary condition for identification as shown in Example 2 where the hidden node has a degree 1 or 2.*

**Remark 3.** *Assumption 3.3 can be further relaxed as demonstrated in the full version [21].*

We start with some definitions. Consider an undirected graph  $\mathcal{G} = (\mathcal{N}, \mathcal{E})$  where  $\mathcal{N} := \{1, \dots, N\}$  is the set of nodes and  $\mathcal{E} \subseteq \mathcal{N} \times \mathcal{N}$  is the set of edges. A *complete* graph is one in which all nodes are adjacent. A subgraph of  $\mathcal{G}$  is a graph  $\mathcal{G}' = (\mathcal{N}', \mathcal{E}')$  with  $\mathcal{N}' \subseteq \mathcal{N}$  and  $\mathcal{E}' \subseteq \mathcal{E}$ . A *clique* of  $\mathcal{G}$  is a complete subgraph of  $\mathcal{G}$ . A *maximal clique* of  $\mathcal{G}$  is a clique that is not a subgraph of another clique of  $\mathcal{G}$ . We say  $\mathcal{G}$  is a *tree* if there is exactly one path between every two nodes. A *forest* is a disjoint union of trees.

For our purposes, an admittance matrix  $Y$  is a complex symmetric matrix (we usually assume  $Y$  satisfies Assumption 3.3). We sometimes refer to  $\mathcal{G}(Y)$  as the *underlying graph* of  $Y$  and write  $\mathcal{G} := (\mathcal{N}, \mathcal{E})$  when  $Y$  is clear from the context. Consider two  $N \times N$  admittance matrices  $Y_1$  and  $Y_2$ . We define two functions of  $(Y_1, Y_2)$  and their underlying graphs. First  $Y_3 := Y_1 + Y_2$  is also an admittance matrix and its underlying

graph  $\mathcal{G}(Y_3) = (\mathcal{N}(Y_3), \mathcal{E}(Y_3))$  is the graph with the same set of nodes and edges in both graphs, i.e.,  $\mathcal{E}(Y_3) := \mathcal{E}(Y_1) \cup \mathcal{E}(Y_2)$ . When the matrices are clear from the context, we also denote the function  $Y_3 = Y_1 + Y_2$  by  $\mathcal{G}_3 = \mathcal{G}_1 \oplus \mathcal{G}_2$ . Note that if  $Y_1$  and  $Y_2$  satisfy Assumption 3.3, so does  $Y_3$ . Second define the  $N \times N$  matrix  $Y_4 := Y_1 \setminus Y_2$  as a function of  $(Y_1, Y_2)$  by:

$$Y_4[i, j] := \begin{cases} Y_1[i, j] & \text{if } i \sim j \text{ and } (i, j) \notin \mathcal{E}_2 \\ -\sum_j Y_4[i, j] & \text{if } i = j \\ 0 & \text{otherwise} \end{cases}$$

The underlying graph  $\mathcal{G}(Y_4)$  is a subgraph of  $\mathcal{G}(Y_1)$  where edges in  $\mathcal{G}(Y_2)$  have been removed. When the matrices are clear from the context, we also denote the function  $Y_4 = Y_1 \setminus Y_2$  by  $\mathcal{G}_4 = \mathcal{G}_1 / \mathcal{G}_2$ . Note that  $Y_4$  satisfies Assumption 3.3 by definition.

Fix an (unknown) admittance matrix  $Y$  and assume its underlying graph  $\mathcal{G} := \mathcal{G}(Y)$  is a tree. Suppose its Kron-reduced admittance matrix  $\bar{Y}$  and its underlying graph  $\bar{\mathcal{G}} := \mathcal{G}(\bar{Y})$  are given. For example  $\bar{Y}$  is obtained according to Corollary 1 from partial voltage and current measurements at measured nodes in  $\mathcal{M}$ .

Next, we will propose a recursive algorithm to recover  $Y$  from  $\bar{Y}$ . Specifically, We can decompose  $\bar{\mathcal{G}}$  to two graphs  $\mathcal{G}_1$  and  $\mathcal{G}_2$  ( $\bar{Y}_1$  and  $\bar{Y}_2$  correspondingly) with distinct properties in Section IV-B1. Secondly, we further introduce a partition of  $Y$  in Section IV-B2 and a corresponding parameterization of  $Y$  in Section IV-B3. Thirdly, we can compute these parameters from known quantity in  $\bar{Y}$  in Section IV-B4. Finally, the overall recursive algorithm to recover  $Y$  is proposed in IV-B5.

1) *Decomposition of  $\bar{\mathcal{G}}$ :* Let  $\bar{\mathcal{E}}_1$  denote the subset of all edges of  $\bar{\mathcal{G}}$  that are between measured nodes in the original graph  $\mathcal{G}$ , and  $\bar{\mathcal{E}}_2$  denote the subset of all edges of  $\bar{\mathcal{G}}$  that have been added by Step 4 of the graph condensation Algorithm 1 when hidden nodes are removed from  $\mathcal{G}$ . By definition of  $\bar{\mathcal{E}}_1, \bar{\mathcal{E}}_2$ , we have  $\bar{\mathcal{G}} = (\mathcal{M}, \bar{\mathcal{E}}_1 \cup \bar{\mathcal{E}}_2)$ .

**Lemma 2.** *Under Assumption 1 and 3,  $\bar{\mathcal{E}}_1 \cap \bar{\mathcal{E}}_2 = \emptyset$ .*

*Proof:* If there exists an edge  $(i, j) \in \bar{\mathcal{E}}_1 \cap \bar{\mathcal{E}}_2$ , then  $(i, j)$  must be an edge in the original graph  $\mathcal{G}$  and nodes  $i$  and  $j$  must also be connected through a path consisting of only hidden nodes. This creates a loop and contradicts that  $\mathcal{G}$  is a tree. Hence  $\bar{\mathcal{E}}_1 \cap \bar{\mathcal{E}}_2 = \emptyset$ . ■

Since  $\bar{\mathcal{G}} = (\mathcal{M}, \bar{\mathcal{E}}_1 \cup \bar{\mathcal{E}}_2)$ , Lemma 2 motivates decomposing  $\bar{\mathcal{G}}$  into two subgraphs,  $\mathcal{G}_1 := (\mathcal{M}, \bar{\mathcal{E}}_1)$  and  $\mathcal{G}_2 := (\mathcal{M}, \bar{\mathcal{E}}_2)$ , both defined on  $\mathcal{M}$  of measured nodes but with disjoint edge sets. While the graph  $\bar{\mathcal{G}} := \mathcal{G}(\bar{Y})$  is defined by the Kron-reduced admittance matrix  $\bar{Y}$ , at this point the graphs  $\mathcal{G}_1, \mathcal{G}_2$  are only defined in terms of the graph  $\bar{\mathcal{G}}$  (in fact in terms of  $\mathcal{G}$ )

and are not associated with any admittance matrices. Define the matrices:

$$\bar{Y}_1 := Y_{11} - \text{diag}\{\mathbf{1}^T Y_{11}\} \quad (16a)$$

$$\bar{Y}_2 := \text{diag}\{\mathbf{1}^T Y_{11}\} - Y_{12} Y_{22}^{-1} Y_{12}^T. \quad (16b)$$

The key observation, stated in the next result, is that  $\mathcal{G}_1, \mathcal{G}_2$  have simple structures, that the matrices defined in (16) are indeed admittance matrices, and that  $\mathcal{G}_1, \mathcal{G}_2$  are the underlying graphs of these admittance matrices. Even though we do not know the submatrices  $Y_{11}, Y_{12}, Y_{22}$  of  $Y$ , the simple structures of  $\mathcal{G}_1, \mathcal{G}_2$  allow us to compute  $\bar{Y}_1, \bar{Y}_2$  as we will see.

**Theorem 1** (Separability). *Suppose the admittance matrix  $Y$  satisfies Assumptions 1, 2 and 3. Then*

1.  $\mathcal{G}_1$  is a forest.
2.  $\mathcal{G}_2 = \oplus_i \mathcal{C}_i$  for some  $\mathcal{C}_i$  are edge-disjoint maximal cliques each with more than 2 nodes.<sup>2</sup>
3.  $\mathcal{G}_1 = \mathcal{G}(\bar{Y}_1)$  and  $\mathcal{G}_2 = \mathcal{G}(\bar{Y}_2)$  so that  $\bar{\mathcal{G}} = \mathcal{G}_1 \oplus \mathcal{G}_2$ .

*Proof:* For the first assertion,  $\mathcal{G}_1$  is a forest since it is a subgraph of the tree  $\mathcal{G}$ . For the second assertion  $\mathcal{G}_2$  is a collection of maximal cliques  $\mathcal{C}_i$  due to Step 4 of the graph condensation Algorithm 1. To show that the maximal clique (in each)  $\mathcal{C}_i$  is of size at least 3, suppose  $\mathcal{C}_i$  consists of  $m_i$  (measured) nodes and, in the original graph  $\mathcal{G}$ , these  $m_i$  measured nodes “surround”  $h_i$  hidden nodes, i.e., the neighbors of each of these hidden nodes are either hidden nodes or nodes in  $\mathcal{C}_i$ . Let  $d_j$  denote the degrees of hidden nodes  $j = 1, \dots, h_i$ . These  $m_i + h_i$  nodes form a (connected) subtree of  $\mathcal{G}$  with exactly  $m_i + h_i - 1$  edges. Since  $m_i$  of these edges are between measured and hidden nodes and  $h_i - 1$  edges are between hidden nodes, we must have  $\sum_{j=1}^{h_i} d_j = m_i + 2(h_i - 1)$  and hence  $m_i = 2 + \sum_{i=1}^{h_i} (d_i - 2)$ . Since  $h_i \geq 1$  and  $d_i \geq 3$  (Assumption 3.2), we have  $m_i \geq 3$ . To show that  $\mathcal{C}_i$  and  $\mathcal{C}_j$  are edge-disjoint, suppose for the sake of contradiction that there is an edge  $(k, l)$  in both  $\mathcal{C}_i$  and  $\mathcal{C}_j$ . By the definition of  $\mathcal{G}_2$ ,  $(k, l)$  is not an edge in the original graph  $\mathcal{G}$ . Since nodes  $k, l$  are both in  $\mathcal{C}_i$ , there is a path from  $k$  to  $l$  in  $\mathcal{G}$  that consists of only hidden nodes connected to measured nodes in the maximal clique  $\mathcal{C}_i$ . Since nodes  $k, l$  are both in  $\mathcal{C}_j$ , there is disjoint path from  $k$  to  $l$  in  $\mathcal{G}$  that consists of a set of hidden nodes connected to nodes in  $\mathcal{C}_j$ . These two paths form a loop in  $\mathcal{G}$ , a contradiction. Hence  $\mathcal{C}_i$  and  $\mathcal{C}_j$  do not share any edge in  $\mathcal{G}_2$ .

For the third assertion, note that the matrix  $\bar{Y}_1$  defined in (16a) is symmetric and hence an admittance matrix. The diagonal entry  $Y_{11}[i, i]$  of  $Y_{11}$  is the negative sum of the off-diagonal entries of the  $i$ th row/column of the original admittance matrix  $Y$  (plus any shunt element at bus  $i$ ), so that the  $i$ th entry of  $\mathbf{1}^T Y_{11}$  is equal to the  $i$ th row sum of  $Y_{12}$  (plus any shunt element at bus  $i$ ). Hence  $\bar{Y}_1$  satisfies Assumption 3.3 if  $Y$  does. Moreover, by the definition of  $\mathcal{G}_1$ , the edges in  $\mathcal{E}_1$  correspond exactly to the off-diagonal entries of  $Y_{11}$  that are

<sup>2</sup>Strictly speaking, each  $\mathcal{C}_i$  is a subgraph of  $\mathcal{G}_2$  with  $\mathcal{M}$  as its node set. It consists of a single maximal clique and the remaining isolated nodes in  $\mathcal{M}$ . We will abuse notation and use  $\mathcal{C}_i$  to both refer to this subgraph of  $\mathcal{G}_2$  and to the maximal clique in  $\mathcal{C}_i$ .

nonzero. This implies that the graph  $\mathcal{G}(\bar{Y}_1)$  that underlies the admittance matrix in (16a) is indeed  $\mathcal{G}_1$ .

The matrix  $\bar{Y}_2$  defined in (16b) is also symmetric and hence is an admittance matrix. If  $Y$  satisfies Assumption 3.3, then

$$\mathbf{1}^T Y_{11} = -\mathbf{1}^T Y_{12}^T, \quad \mathbf{1}^T Y_{12} = -\mathbf{1}^T Y_{22}.$$

This implies

$$\text{diag}\{\mathbf{1}^T Y_{11}\} = \text{diag}\{\mathbf{1}^T Y_{12} Y_{22}^{-1} Y_{12}^T\},$$

i.e.,  $\bar{Y}_2$  defined in (16b) satisfies Assumption 3.3 when  $Y$  does.

Next we show that  $\mathcal{G}_2 = \mathcal{G}(\bar{Y}_2)$ . From (16)

$$\bar{Y} = Y_{11} - Y_{12} Y_{22}^{-1} Y_{12}^T = \bar{Y}_1 + \bar{Y}_2,$$

and hence  $\bar{\mathcal{G}} := \mathcal{G}(\bar{Y}) = \mathcal{G}_1 \oplus \mathcal{G}_2$  with  $\mathcal{G}(\bar{Y}_1) = \mathcal{G}_1$ . Therefore we have  $\mathcal{G}(\bar{Y}_2) = \mathcal{G}_2$ . This concludes the proof. ■

**Remark 4.** *From the third assertion, we have shown that, once  $\mathcal{G}_1$  and  $\mathcal{G}_2$  are obtained from  $\mathcal{G}, \bar{Y}_1$  and  $\bar{Y}_2$  defined in (16) can be obtained.*

There are many algorithms for solving the clique problem, such as the Bron-Kerbosch algorithm, which we adopt in Algorithm 2.

---

#### Algorithm 2 Graph Decoupling Algorithm

---

- 1: **Input:** a condensed graph  $\bar{\mathcal{G}}$
  - 2: Set  $\mathcal{G}' = \bar{\mathcal{G}}, i = 1$ .
  - 3: **while**  $\mathcal{G}'$  has a clique with more than two nodes **do**
  - 4:   Use Bron-Kerbosch Algorithm to find a clique ( $\geq 3$  nodes, together with other isolating nodes)  $\mathcal{C}_i$  in  $\mathcal{G}'$ ,
  - 5:   Let  $\mathcal{G}' = \mathcal{G}' / \mathcal{C}_i, i = i + 1$ ,
  - 6: **end while**
  - 7: **return**  $\mathcal{G}_2 = \oplus_i \mathcal{C}_i, \mathcal{G}_1 = \bar{\mathcal{G}} / \mathcal{G}_2$  and the corresponding  $\bar{Y}_1$  and  $\bar{Y}_2$ .
- 

2) *Partition of  $Y$ :* Next we propose an algorithm to obtain  $Y_{11}, Y_{22}$  and  $Y_{12}$ , and therefore the original admittance matrix  $Y$ .

The decomposition of  $\bar{\mathcal{G}}$  into  $\mathcal{G}_1$  and  $\mathcal{G}_2$  guaranteed by Theorem 1 allows us to partition the set  $\mathcal{M}$  into a subset of *internal* measured nodes that are not connected to any hidden nodes and a disjoint subset of *boundary* measured nodes that connect to some hidden nodes. We can similarly partition  $\mathcal{H}$  into a subset of *internal* hidden nodes that are not connected to any measured nodes and the disjoint subset of *boundary* hidden nodes that connect to some measured nodes. The decomposition of  $\bar{\mathcal{G}}$  into  $\mathcal{G}_1$  and  $\mathcal{G}_2$  identifies only the types of measured nodes, but not those of hidden nodes. We can hence arrange the original admittance matrix  $Y$  into the following structure (only the upper triangular submatrix is shown as  $Y$  is symmetric):

$$Y = \left[ \begin{array}{c|c} Y_{11} & Y_{12} \\ \hline & Y_{22} \end{array} \right] =: \left[ \begin{array}{cc|cc} Y_{11,11} & Y_{11,12} & 0 & 0 \\ & Y_{11,22} & Y_{12,21} & 0 \\ \hline & & Y_{22,11} & Y_{22,12} \\ & & & Y_{22,22} \end{array} \right]. \quad (17a)$$

Here, for  $Y_{11}$ , the submatrix  $Y_{11,11}$  corresponds to connectivity among the internal measured nodes,  $Y_{11,22}$  corresponds to

connectivity among the boundary measured nodes, and  $Y_{11,12}$  corresponds to connectivity between the internal and boundary measured nodes. Similarly, for  $Y_{22}$ , the submatrix  $Y_{22,11}$  corresponds to connectivity among the boundary hidden nodes,  $Y_{22,22}$  to that among the internal hidden nodes, and  $Y_{22,12}$  to that between the internal and boundary hidden nodes. The submatrix  $Y_{12,21}$  corresponds to connectivity between the set of boundary measured nodes and the set of boundary hidden nodes. Denote the inverse  $Y_{22}^{-1}$  by:

$$X_{22} := Y_{22}^{-1} =: \begin{bmatrix} X_{22,11} & X_{22,12} \\ X_{22,12}^T & X_{22,22} \end{bmatrix}.$$

We have

$$\begin{aligned} \bar{Y} &= Y_{11} - Y_{12}Y_{22}^{-1}Y_{12}^T \\ &= \begin{bmatrix} Y_{11,11} & Y_{11,12} \\ Y_{11,12}^T & Y_{11,22} \end{bmatrix} - \begin{bmatrix} 0 & 0 \\ 0 & Y_{12,21}X_{22,11}Y_{12,21}^T \end{bmatrix}, \end{aligned} \quad (17b)$$

where  $X_{22,11} = (Y_{22,11} - Y_{22,12}Y_{22,22}^{-1}Y_{22,12}^T)^{-1}$  from (17a) and the Woodbury formula. Specifically, given the definition of Schur complement

$$\det(Y_{22,11} - Y_{22,12}Y_{22,22}^{-1}Y_{22,12}^T) \det Y_{22,22} = \det Y_{22},$$

and from the invertibility of  $Y_{22}$  (shown in Proposition 2), the right-hand side of the above equation is nonzero. Therefore  $\det(Y_{22,11} - Y_{22,12}Y_{22,22}^{-1}Y_{22,12}^T)$  cannot be zero, and as a result, the invertibility of  $X_{22,11}$  can be guaranteed.

Since we can compute  $\bar{Y}$  from partial voltage and current measurements, we can identify submatrices  $Y_{11,11}$  and  $Y_{11,12}$  for internal measured nodes from  $\bar{Y}$  according to (17b). The edges in  $\mathcal{E}_1$  correspond to the off-diagonal entries of  $[Y_{11,11} \ Y_{11,12}]$  as well as  $Y_{11,12}^T$ , and they form a forest (Theorem 1). The edges in  $\mathcal{E}_2$  correspond to the off-diagonal entries of  $Y_{11,22} - Y_{12,21}X_{22,11}Y_{12,21}^T$ , and they form a collection of cliques. Recall that both  $\mathcal{G}_1$  and  $\mathcal{G}_2$  have  $\mathcal{M}$  as their node set; see the example in Fig. 3.

In the rest of this subsection we focus on identifying the remaining submatrices  $Y_{11,22}$ ,  $Y_{12,21}$  as well as  $Y_{22}$  (or specifically,  $Y_{22,11}$ ,  $Y_{22,12}$ ,  $Y_{22,22}$ ) of  $Y$ . For this purpose we assume without loss of generality that all measured nodes are boundary measured nodes, i.e., the rows and columns corresponding to submatrices  $Y_{11,11}$  and  $Y_{11,12}$  as well as their contributions to the diagonal entries of  $Y_{11,22}$  have been removed from  $Y$ . Then

$$Y = \left[ \begin{array}{c|c} Y_{11} & Y_{12} \\ \hline & Y_{22} \end{array} \right] =: \left[ \begin{array}{c|cc} Y_{11,22} & Y_{12,21} & 0 \\ \hline & Y_{22,11} & Y_{22,12} \\ & & Y_{22,22} \end{array} \right]. \quad (18)$$

Our goal is to identify  $Y$  in (18) given its Kron-reduction:

$$\bar{Y} = Y_{11,22} - Y_{12,21}X_{22,11}Y_{12,21}^T.$$

Theorem 1.2 implies that the underlying Kron-reduce graph  $\mathcal{G}(\bar{Y})$  is a disjoint collection of maximal cliques  $\mathcal{C}_i$  among boundary measured nodes. By *hidden nodes in a maximal clique  $\mathcal{C}_i$*  of the Kron-reduced graph  $\mathcal{G}$ , we mean the nonempty set of hidden nodes in the original graph  $\mathcal{G}$  that are connected either to the measured nodes in  $\mathcal{C}_i$  or other hidden nodes in  $\mathcal{C}_i$ . A measured node can be in multiple cliques  $\mathcal{C}_i$  though  $\mathcal{C}_i$  are edge-disjoint (Theorem 1.2).

**Lemma 3.** *Suppose the admittance matrix  $Y$  satisfies Assumptions 1, 2 and 3. A measured node can connect to only one hidden node in any cliques  $\mathcal{C}_i$  of which it is a member.*

*Proof:* If a measured node connects to more than one hidden node in a maximal cliques  $\mathcal{C}_i$ , there exists a loop since there is a path between any two hidden nodes in  $\mathcal{C}_i$ , hence a contradiction. ■

We further assume, without loss of generality, that  $\mathcal{G}(\bar{Y})$  consists of a single clique; otherwise, we can repeatedly apply Algorithm 3 below to each clique separately to determine the corresponding submatrices and then combine them to obtain  $Y_{22}$  and  $Y_{12}$ . The general case has been discussed and elaborated in the Appendix.

**Remark 5.** *With this further assumption, Lemma 3 guarantees that  $Y_{12}$  has exactly one nonzero element in each row.*

3) *Parameterization of  $Y$ :* Recall that there are  $M$  (boundary) measured nodes, indexed by  $1, \dots, M$ , so that  $Y_{11,22}$  in (18) is  $M \times M$ . Suppose there are  $H_b$  boundary hidden nodes, indexed by  $M+1, \dots, M+H_b$ , and  $H_i := H - H_b$  internal hidden nodes, indexed by  $M+H_b+1, \dots, M+H$ . Then  $Y_{22,11}$  in (18) is  $H_b \times H_b$  and  $Y_{22,22}$  is  $H_i \times H_i$ . Suppose each measured node  $i \in \{1, \dots, M\}$  is connected to the hidden node  $h(i) \in \{M+1, \dots, M+H_b\}$  by a line with series admittance  $y_{ih(i)}$ . From Remark 5 we know there is a unique  $h(i)$  for each  $i$ , but voltage and current measurements only identify the identity of each measured node  $i$ , but not the hidden node  $h(i)$  it is connected to (nor the values of  $H, H_b, H_i$ ). The next result suggests a method to identify all measured nodes that are connected to the same boundary hidden node.

**Proposition 3.** *Suppose the admittance matrix  $Y$  satisfies Assumptions 1, 2 and 3. Two measured nodes  $i$  and  $j$  are connected to the same hidden node if and only if the off-diagonal entries of rows  $i$  and  $j$  of  $\bar{Y}_2$  are proportional, i.e., there exists  $\gamma(i, j) \neq 0$  such that*

$$\frac{\bar{Y}_2[i, k]}{\bar{Y}_2[j, k]} = \gamma(i, j), \quad k \neq i, j, k = 1, \dots, M.$$

*Proof:* As discussed above, each row of  $Y_{12,21}$  has exactly a single nonzero entry. For each measured node  $i$ , let  $h(i)$  denote the hidden node to which  $i$  is adjacent and  $y_{ih(i)}$  denotes the series admittance of line  $(i, h(i))$ . Then

$$Y_{12,21} =: \begin{bmatrix} -y_{1h(1)}e_{h(1)}^T \\ \vdots \\ -y_{Mh(M)}e_{h(M)}^T \end{bmatrix}$$

where the unit vector  $e_i \in \{0, 1\}^{H_b}$  is the column vector with a single 1 in the  $i$ th entry and 0 elsewhere. Denote the  $(i, j)$ th entry of  $X_{22,11}$  by  $\beta_{ij}$ . Then the  $i$ th row of matrix  $Y_{12,21}X_{22,11}Y_{12,21}^T$  in (16b) is

$$y_{ih(i)} [\beta_{h(i)h(1)}y_{1h(1)} \cdots \beta_{h(i)h(M)}y_{Mh(M)}].$$

The **necessity** of the proposition can be proven as follows: if  $i$  and  $j$  are connected to the same hidden node, i.e.,  $h(i) =$



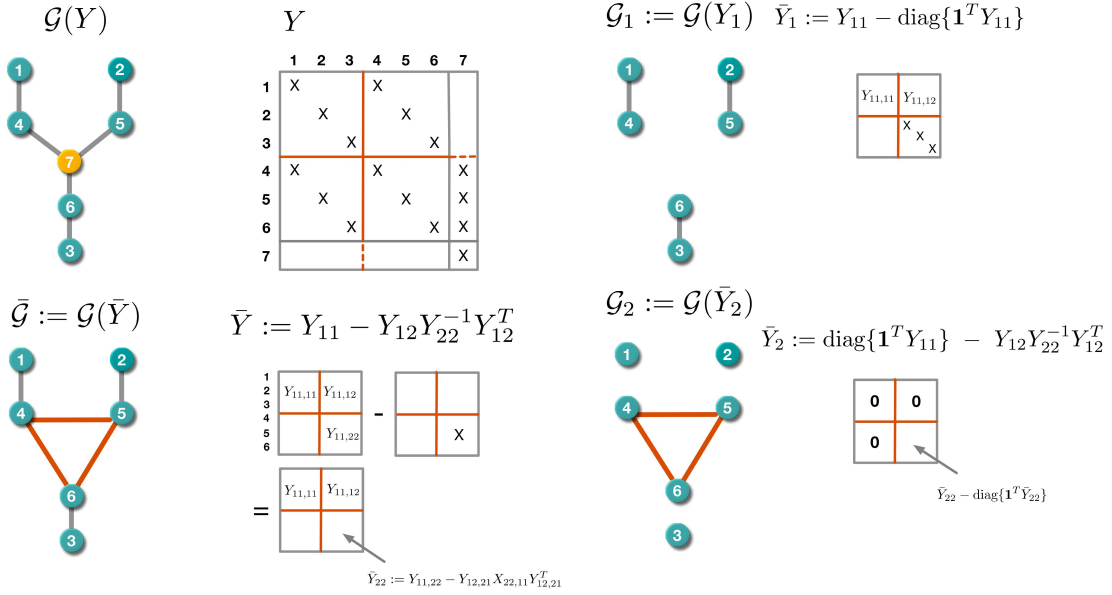


Fig. 3. Illustration of admittance matrices and their underlying graphs:  $(Y, \mathcal{G}(Y))$ ,  $(\bar{Y}, \bar{\mathcal{G}})$ ,  $(\bar{Y}_1, \mathcal{G}_1)$ , and  $(\bar{Y}_2, \mathcal{G}_2)$ .

$h(i)$ , then  $b_{h(j)}^\top = b_{h(i)}^\top$ . Therefore, for  $k \neq i, j$ , we have from (16b)

$$\bar{Y}_2[i, k] = \gamma(i, j) \bar{Y}_2[j, k]$$

for  $\gamma(i, j) := y_{ih(i)}/y_{jh(j)}$ .

We now present the **sufficiency** proof. Fix  $i \neq j$ , and suppose there exists  $\gamma'(i, j) \neq 0$  such that  $\bar{Y}_2[i, k] = \gamma'(i, j) \bar{Y}_2[j, k]$  for all  $k \neq i, j$ . Then

$$\gamma \beta_{h(i)h(k)} = \beta_{h(j)h(k)}, \quad k \neq i, j \quad (19)$$

where  $\gamma := y_{ih(i)}/(\gamma'(i, j)y_{jh(j)})$ . We have to prove that  $h(i) = h(j)$ .

Suppose  $h(i) \neq h(j)$ . Assume without loss of generality that  $h(i) = 1$  and  $h(j) = 2$  (corresponding to nodes  $M+1$  and  $M+2$  respectively). By Assumptions 3.3,  $Y$  is symmetric and hence  $\bar{Y}$ ,  $X_{22} := Y_{22}^{-1}$ , and  $X_{22,11}$  are symmetric. Then (19) means that the matrix  $X_{22,11}$  is of the form

$$X_{22,11} = \begin{bmatrix} \beta_{11} & \beta_{12} & \beta_{13} & \cdots & \beta_{1H_b} \\ \beta_{12} & \beta_{22} & \gamma\beta_{13} & \cdots & \gamma\beta_{1H_b} \\ \beta_{13} & \gamma\beta_{13} & \beta_{33} & \cdots & \beta_{3H_b} \\ \vdots & \vdots & \vdots & \ddots & \vdots \\ \beta_{1H_b} & \gamma\beta_{1H_b} & \beta_{3H_b} & \cdots & \beta_{H_b H_b} \end{bmatrix} \quad (20a)$$

$$=: \begin{bmatrix} A_{11} & A_{12} \\ A_{12}^\top & A_{22} \end{bmatrix}. \quad (20b)$$

In particular  $\text{rank}(A_{12}) \leq 1$ . Suppose more than one measured nodes are connected to each of the hidden nodes  $h(i)$  and  $h(j)$ . Specifically let  $h(i) = h(i')$  and  $h(j) = h(j')$  for distinct  $i', j'$ . Then letting  $k = i'$  and then  $k = j'$  in (19) implies that

$$\beta_{h(i)h(i)} = \beta_{h(i)h(i')} = \frac{1}{\gamma} \beta_{h(j)h(i')} = \frac{1}{\gamma} \beta_{h(j)h(i)}$$

$$\beta_{h(j)h(j)} = \beta_{h(j)h(j')} = \gamma \beta_{h(i)h(j')} = \gamma \beta_{h(i)h(j)}.$$

This implies that  $\beta_{21} = \beta_{12} = \gamma\beta_{11}$  and  $\beta_{22} = \gamma\beta_{12}$  in (20a),

i.e., the first two rows of  $X_{22,11}$  are linearly dependent. This contradicts the invertibility of  $X_{22,11}$  and hence  $h(i) = h(j)$  if more than one measured nodes are connected to each of  $h(i)$  and  $h(j)$ .

Suppose then at least one of  $h(i)$ ,  $h(j)$  is connected to a single measured node (i.e.,  $i$  or  $j$ ) so that  $\gamma\beta_{h(i)h(k)} = \beta_{h(j)h(k)}$  in (19) may not hold for  $k = i$  or  $k = j$  or both. Let

$$X_{22,11}^{-1} =: \begin{bmatrix} B_{11} & B_{12} \\ B_{12}^\top & B_{22} \end{bmatrix} \quad (21)$$

where  $B_{11} \in \mathbb{C}^{2 \times 2}$  and  $B_{22} \in \mathbb{C}^{(H_b-2) \times (H_b-2)}$ .

We now prove  $\text{rank}(B_{12}) \leq 1$  through direct calculation. We then derive a contradiction first for the case when  $\text{rank}(B_{12}) = 0$  and then when  $\text{rank}(B_{12}) = 1$ . This implies that  $h(i) = h(j)$ , i.e.,  $i$  and  $j$  are connected to the same (boundary) hidden node.

**Proof of  $\text{rank}(B_{12}) \leq 1$ .** From (20) and (21), the entries of  $B_{12}$  are given by: for  $k \geq 3$ ,

$$[B_{12}]_{1k} = \frac{(-1)^{k+1}}{\det(X_{22,11})} \begin{vmatrix} \beta_{12} & b^\top \\ \beta_{22} & \gamma b^\top \\ \gamma c_{-k} & B_{-k} \end{vmatrix} \quad (22a)$$

$$[B_{12}]_{2k} = \frac{(-1)^k}{\det(X_{22,11})} \begin{vmatrix} \beta_{11} & b^\top \\ \beta_{12} & \gamma b^\top \\ c_{-k} & B_{-k} \end{vmatrix} \quad (22b)$$

where  $b^\top$  is the first row of  $A_{12}$ ,  $c_{-k}$  is the  $H_b-3$  dimensional (column) vector which is the first column of  $A_{12}^\top$  with its  $k$ th entry removed, and  $B_{-k}$  is the  $(H_b-3) \times (H_b-2)$  matrix which is  $A_{22}$  with its  $k$ th row removed. For ease of reference we state the following calculation as a lemma without proof.

**Lemma 4.** Given any scalars  $\alpha, \beta, \gamma \in \mathbb{C}$ , any column vectors  $b, c$ , and any matrix  $B$  of matching sizes, we have the following

determinant

$$\begin{vmatrix} \alpha & b^\top \\ \beta & \gamma b^\top \\ c & B \end{vmatrix} = (\gamma\alpha - \beta) \begin{vmatrix} b^\top \\ B \end{vmatrix}.$$

Applying Lemma 4 to (22) we have

$$\begin{aligned} [B_{12}]_{1k} &= (-1)^{k+1} a_1 d_k, & k \geq 3 \\ [B_{12}]_{2k} &= (-1)^k a_2 d_k, & k \geq 3 \end{aligned}$$

where

$$a_1 := \frac{\gamma\beta_{12} - \beta_{22}}{\det(X_{22,11})}, \quad a_2 := \frac{\gamma\beta_{11} - \beta_{12}}{\det(X_{22,11})}, \quad d_k := \begin{vmatrix} b^\top \\ B_{-k} \end{vmatrix}$$

i.e.,  $B_{12}$  is of the form

$$B_{12} = \begin{bmatrix} a_1 d_3 & -a_1 d_4 & \cdots & (-1)^{H_b-1} a_1 d_{H_b-2} \\ -a_2 d_3 & a_2 d_4 & \cdots & (-1)^{H_b} a_2 d_{H_b-2} \end{bmatrix} \quad (23)$$

This shows that  $\text{rank}(B_{12}) \leq 1$ .

**Case 1:  $\text{rank}(B_{12}) = 0$ .** The key observation is that,  $X_{22,11}^{-1} = Y_{22}/Y_{22,22}$  is the admittance matrix of the Kron-reduced network consisting of only boundary hidden nodes where two boundary hidden nodes  $h(k)$  and  $h(k')$  are adjacent if and only if, in the original network,  $h(k)$  and  $h(k')$  are either adjacent or are connected by a path with only internal hidden nodes (even though  $Y_{22}$  may not have zero row sums because each diagonal entry of  $Y_{22}$  may include line admittances that can be interpreted as a shunt admittance in the Kron-reduced network). Note that  $h(k)$  and  $h(k')$  cannot both be adjacent and connected by a path with only internal hidden nodes because, otherwise, there is a loop in the original network. Then  $B_{12}$  describes the connectivity of nodes  $h(i)$ ,  $h(j)$  with other boundary hidden nodes in the Kron-reduced network.

When  $\text{rank}(B_{12}) = 0$  (either  $a_1 = a_2 = 0$  or  $d_k = 0$  for all  $k \geq 3$  in (23)), then  $h(i)$  and  $h(j)$  are connected at most to each other in the Kron-reduced network represented by  $Y_{22}/Y_{22,22}$ . If either  $h(i)$  or  $h(j)$  is connected to a single measured node, this violates Assumptions 3.2 that every hidden node has degree at least 3 in the original (not Kron-reduced) network.

**Case 2:  $\text{rank}(B_{12}) = 1$ .** Then either  $a_1 > 0$  or  $a_2 > 0$ , or both. Suppose one of  $h(i) = 1$  and  $h(j) = 2$ , say,  $h(i)$  is connected to more than one measured node (and  $h(j)$  is connected to a single measured node). The argument above shows that  $\gamma\beta_{h(i)h(i)} = \beta_{h(j)h(i)} = \beta_{h(i)h(j)}$  and hence  $a_2 = 0$  and  $[B_{12}]_{2k} = 0$  for all  $k \geq 3$ . This means that  $h(j) = 2$  is connected only to a single measured node and at most the boundary hidden node  $h(i)$  in the Kron-reduced network represented by  $Y_{22}/Y_{22,22}$ , violating Assumptions 3.2 that every hidden node has degree at least 3 in the original network.

Suppose then both  $h(i)$  and  $h(j)$  are connected to a single measured node each. Then  $a_1 > 0$  and  $a_2 > 0$  because otherwise, either  $[B_{12}]_{1k} = 0$  or  $[B_{12}]_{2k} = 0$  for all  $k \geq 3$ , violating Assumptions 3.2. But (23) implies that  $[B_{12}]_{1k} \neq 0$  if and only if  $[B_{12}]_{2k} \neq 0$ , i.e.,  $h(i)$  and  $h(j)$  are connected to exactly the same set of boundary hidden nodes in the Kron-reduced network represented by  $Y_{22}/Y_{22,22}$ . If  $h(i)$  and  $h(j)$

are connected to each other and no common boundary hidden node or if they are connected to only 1 common hidden node (and not to each other), then Assumptions 3.2 is violated. If they are connected to 2 or more common boundary hidden nodes, then there must be a loop in the original (not Kron-reduced) network, violating Assumptions 3.1.

This completes the proof of sufficiency.  $\blacksquare$

Note that if there are only  $M = 3$  measured nodes then Assumptions 3.1 and 3.2 imply that all of them must be connected to the same boundary hidden node.

Given the Kron-reduced admittance matrix  $\bar{Y}_2$ , Proposition 3 allows us to group together the (boundary) measured nodes that are connected to the same (boundary) hidden node. This also identifies the number of boundary hidden nodes, even though we do not know (yet) the number or identity of internal hidden nodes nor the connectivity among the nodes. We can re-arrange the submatrix matrix  $Y_{12,21}$  into a form easier for identification.

Specifically let measured nodes  $1, \dots, k_1$  be connected to hidden node  $M + 1$ , measured nodes  $k_1 + 1, \dots, k_2$  to hidden node  $M + 2, \dots$ , measured nodes  $k_{H_b-1} + 1, \dots, k_{H_b} := M$  to hidden node  $M + H_b$ . Note that Proposition 3 yields the values for  $H_b$  and  $(k_1, k_2, \dots, k_{H_b} = M)$  even though it provides no information about the value of  $H$ , the total number of hidden nodes. To simplify notation, denote the series admittance  $y_{ih(i)}$  of line  $(i, h(i))$  by  $y_i$ . Then  $Y_{12} = [Y_{12,21} \ 0]$  where  $Y_{12,21}$  is  $M \times H_b$  and can be arranged into the following simple form:

$$Y_{12,21} = \begin{bmatrix} -y_1 & 0 & \cdots & 0 \\ \vdots & \vdots & \vdots & \vdots \\ -y_{k_1} & 0 & \cdots & 0 \\ 0 & -y_{k_1+1} & \cdots & 0 \\ \vdots & \vdots & \vdots & \vdots \\ 0 & -y_{k_2} & \cdots & 0 \\ \vdots & \vdots & \vdots & \vdots \\ 0 & 0 & \cdots & -y_{k_{H_b}} \end{bmatrix} =: \begin{bmatrix} -\hat{y}_1 & 0 & \cdots & 0 \\ 0 & -\hat{y}_2 & \cdots & 0 \\ \vdots & \vdots & \ddots & \vdots \\ 0 & 0 & \cdots & -\hat{y}_{H_b} \end{bmatrix},$$

where for  $i = 1, \dots, H_b$ ,  $\hat{y}_i$  is a  $(k_i - k_{i-1})$ -dimensional column vector corresponding to  $k_i - k_{i-1}$  measured nodes that are connected to the hidden node  $M + i$ . Since  $Y$  has zero row sum by Assumption 3.3, the diagonal matrix  $\text{diag}\{\mathbf{1}^T Y_{11}\} = \text{diag}\{\mathbf{1}^T Y_{11,22}\} = \text{diag}(y_i = y_{ih(i)}, i = 1, \dots, M)$ . We have

$$\begin{aligned} & Y_{12} Y_{22}^{-1} Y_{12}^T \\ &= \text{diag}(\hat{y}_j) X_{22,11} \text{diag}(\hat{y}_j^T) \\ &= \begin{bmatrix} \beta_{11} \hat{y}_1 \hat{y}_1^T & \beta_{12} \hat{y}_1 \hat{y}_2^T & \cdots & \beta_{1H_b} \hat{y}_1 \hat{y}_{H_b}^T \\ \beta_{21} \hat{y}_2 \hat{y}_1^T & \beta_{22} \hat{y}_2 \hat{y}_2^T & \cdots & \beta_{2H_b} \hat{y}_2 \hat{y}_{H_b}^T \\ \vdots & \vdots & \ddots & \vdots \\ \beta_{H_b,1} \hat{y}_{H_b} \hat{y}_1^T & \beta_{H_b,2} \hat{y}_{H_b} \hat{y}_2^T & \cdots & \beta_{H_b,H_b} \hat{y}_{H_b} \hat{y}_{H_b}^T \end{bmatrix}. \end{aligned}$$

Then the admittance matrix corresponding to the graph  $\mathcal{G}_2$  in

Theorem 1 is:

$$\bar{Y}_2 = \begin{bmatrix} \text{diag}(\hat{y}_1) & 0 & \cdots & 0 \\ & \text{diag}(\hat{y}_2) & \cdots & 0 \\ & & \ddots & \vdots \\ & & & \text{diag}(\hat{y}_M) \end{bmatrix} - \begin{bmatrix} \beta_{11} \hat{y}_1 \hat{y}_1^T & \beta_{12} \hat{y}_1 \hat{y}_2^T & \cdots & \beta_{1H_b} \hat{y}_1 \hat{y}_{H_b}^T \\ & \beta_{22} \hat{y}_2 \hat{y}_2^T & \cdots & \beta_{2H_b} \hat{y}_2 \hat{y}_{H_b}^T \\ & & \ddots & \vdots \\ & & & \beta_{H_b H_b} \hat{y}_{H_b} \hat{y}_{H_b}^T \end{bmatrix}. \quad (24)$$

Recall that we have already identified the Kron-reduced admittance matrix  $\bar{Y}_2$ , i.e., we know every entry of  $\bar{Y}_2$  on the left-hand side of (24). We now explain how to identify  $(\beta_{ij}, i, j = 1, \dots, H_b)$  and  $(y_i = y_{ih(i)}, i = 1, \dots, M)$  on the right-hand side of (24). In particular,  $(y_i = y_{ih(i)}, i = 1, \dots, M)$  yields  $Y_{12}$  of the original admittance matrix  $Y$ .

4) *Computation of parameters in  $Y$* : Let  $\bar{Y}_{2,k_1}$  be the diagonal submatrix consisting of the first  $k_1$  rows and columns of  $\bar{Y}_2$  corresponding to the first  $k_1$  measured nodes connected to the first hidden node  $M+1$ :

$$\begin{aligned} \bar{Y}_{2,k_1} &:= \text{diag}(\hat{y}_1) - \beta_{11} \hat{y}_1 \hat{y}_1^T \\ &= \begin{bmatrix} y_1 & \cdots & 0 \\ & \ddots & \vdots \\ & & y_{k_1} \end{bmatrix} - \beta_{11} \begin{bmatrix} y_1 \\ \vdots \\ y_{k_1} \end{bmatrix} \begin{bmatrix} y_1 & \cdots & y_{k_1} \end{bmatrix}. \end{aligned} \quad (25)$$

We first explain how to identify  $(\beta_{11}, \hat{y}_1)$  on the right-hand side of (25) from the knowledge of  $\bar{Y}_{2,k_1}$  on the left-hand side of (25). The identification of other  $\beta_{ii}, \hat{y}_i$  corresponding to  $k_i - k_{i-1}$  measured nodes connected to the hidden node  $M+i$  from the diagonal blocks  $\bar{Y}_{2,k_i} := \text{diag}(y_{k_{i-1}-1}, \dots, y_{k_i}) - \beta_{ii} \hat{y}_i \hat{y}_i^T$  can be done similarly.

*Case 1:  $k_1 \geq 2$* . In this case, hidden node  $M+1$  is connected to two or more measured nodes indexed by  $i = 1, \dots, k_1$ . Consider the first two measured nodes and the corresponding  $2 \times 2$  principal submatrix of  $Y_{2,k_1}$ : for  $i, j = 1, 2$

$$\bar{Y}_{2,k_1}[i, j] = \begin{cases} y_i - \beta_{11} y_i^2 & \text{if } i = j \\ -\beta_{11} y_i y_j & \text{if } i \neq j \end{cases} \quad (26)$$

This leads to the following equations in  $(\beta_{11}, y_1, y_2)$ :

$$\begin{aligned} y_1 - \beta_{11} y_1^2 &= \bar{Y}_{2,k_1}[1, 1] =: a_1 \\ -\beta_{11} y_1 y_2 &= \bar{Y}_{2,k_1}[1, 2] =: a_2 \\ y_2 - \beta_{11} y_2^2 &= \bar{Y}_{2,k_1}[2, 2] =: a_3 \end{aligned}$$

yielding:

$$\begin{aligned} y_1 &= \frac{a_1 a_3 - a_2^2}{a_2 + a_3}, \quad y_2 = \frac{a_1 a_3 - a_2^2}{a_1 + a_2}, \\ \beta_{11} &= -\frac{a_2(a_1 + a_2)(a_2 + a_3)}{(a_1 a_3 - a_2^2)^2}. \end{aligned} \quad (27)$$

To identify other  $(y_j, j > 2)$ , note that

$$-\beta_{11} y_1 y_j = Y_{2,k_1}[1, j], \quad j = 3, \dots, k_1$$

yielding

$$y_j = -\frac{Y_{2,k_1}[1, j]}{\beta_{11} y_1},$$

where  $\beta_{11}$  and  $y_1$  are given by (27). Once  $\hat{y}_1, \dots, \hat{y}_{k_1}$  are found, we can calculate from off-diagonal entries of  $Y_2$  all  $\beta_{ij}$  from (24).

*Case 2*: Once we have recovered the coefficients for hidden boundary nodes with at least two connections to measured nodes in Case 1, next, we can treat these recovered hidden nodes as measured nodes and repeat the above procedure until no hidden node is left. A key step is to construct a new Kron reduced matrix once parts of the admittance matrix have been found. Let the original  $Y$  have the following partition as in (18):

$$Y = \left[ \begin{array}{c|cc} Y_{11,22} & Y_{12,21} & 0 \\ \hline Y_{22,11} & Y_{22,12} & \\ & Y_{22,22} & \end{array} \right].$$

The Kron reduced admittance matrix can be decomposed to  $\bar{Y}_1$  and  $\bar{Y}_2$ . Specifically,  $\bar{Y}_2$  has the following form:

$$\begin{aligned} \bar{Y}_2 &= \text{diag}\{\mathbf{1}^T Y_{11,22}\} - Y_{12,21} X_{22,11} Y_{12,21}^T \\ &= \text{diag}\{\mathbf{1}^T Y_{11,22}\} - [Y_{12,21} \quad 0] \begin{bmatrix} Y_{22,11} & Y_{22,12} \\ Y_{22,12}^T & Y_{22,22} \end{bmatrix}^{-1} \begin{bmatrix} Y_{12,21}^T \\ 0 \end{bmatrix}. \end{aligned}$$

Based on the results in Case 1, one can recover  $\text{diag}\{\mathbf{1}^T Y_{11,22}\}$ ,  $Y_{12,21}$  and  $X_{22,11}$ . Since  $\bar{Y}_1$  is known from Algorithm 2,  $\text{diag}\{\mathbf{1}^T Y_{11,22}\}$  allows us to compute  $Y_{11}$  from the equality (16a) and the partition in (18):

$$Y_{11} = \bar{Y}_1 + \text{diag}\{\mathbf{1}^T Y_{11,22}\}. \quad (28)$$

Hence the entire rows and columns of  $Y$  corresponding to the boundary measured nodes are known after (28). We can then focus on the submatrices  $Y_{22,11}$ ,  $Y_{22,12}$ ,  $Y_{22,22}$  corresponding to only the boundary and internal hidden nodes, i.e., we can reduce the unknown admittance matrix  $Y$  to the new smaller admittance matrix below, which amounts to restricting attention to the subgraph without the boundary measured nodes.

$$Y = \left[ \begin{array}{c|c} Y_{22,11} & Y_{22,12} \\ \hline & Y_{22,22} \end{array} \right].$$

The Kron reduced admittance matrix of this new (unknown) admittance matrix  $Y$  can then be obtained from the knowledge of  $X_{22,11}$ :

$$\bar{Y} := Y_{22,11} - Y_{22,12} Y_{22,22}^{-1} Y_{22,12}^T = X_{22,11}^{-1}.$$

Moreover, we have identified the set of boundary hidden nodes. Applying Theorem 1, Algorithm 2 and Proposition 3 to this new  $\bar{Y}$  allows us to identify a set of internal hidden nodes to which this set of boundary hidden nodes are connected. Moreover, we can treat the set of boundary hidden nodes as boundary measured nodes and the newly identified internal hidden nodes as boundary hidden nodes. Therefore, even though we do not know the number or the identity of the *remaining* internal hidden nodes, we can partition the new (unknown) admittance matrix  $Y$  into the form at the beginning of Case 2 and therefore repeat the computation on this new (smaller) admittance matrix recursively, strictly reducing the

number of internal hidden nodes in each iteration until the set of internal hidden nodes becomes null.

*Case 3:* For any hidden node that connects to one or zero measured node, these hidden nodes will eventually have more than one connection to measured nodes once the other hidden nodes have been recovered and therefore can be recovered. It is easy to show that there will never exist a scenario that all the hidden nodes have at most 1 connection to measured nodes for a tree graph. To see this, note that for any clique,  $H \geq M$  as every hidden node connects to a different measured node. On one hand, the sum of all hidden nodes' degrees is greater than  $3H$  under Assumption 3. On the other hand, it is at most  $2(H - 1) + M$ , which is twice the sum of all edges between hidden nodes and the number of connections between hidden nodes and measured nodes. However,  $2(H - 1) + M < 3H$ , a contradiction.

*Case 4:* If all hidden nodes are hidden boundary nodes, i.e.,  $Y_{22} = Y_{22,11}$ , then  $Y_{22} = X_{22,11}^{-1}$  and hence the entire admittance matrix  $Y$  can be identified. If there are hidden nodes that are not hidden boundary nodes, we can treat hidden boundary nodes as measured nodes now and repeat the above procedure based on Case 2.

5) *Overall recursive algorithm:* The overall identification procedure is summarized in Algorithm 3<sup>3</sup>.

---

#### Algorithm 3 Recover $Y$ from $\bar{Y}$

---

- 1: **Input:**  $\bar{Y}_1$  and  $\bar{Y}_2$
  - 2: **for** each pair of nodes  $(j, k)$  **do**
  - 3:   Compute  $\gamma[j, k]$  from  $\bar{Y}_2$ .
  - 4: **end for**
  - 5: Solve for  $\text{diag}\{\mathbf{1}^T Y_{11,22}\}$ ,  $Y_{12,21}$  and  $X_{22,11}$  from (25),  
 set  $\hat{Y} = \begin{bmatrix} \bar{Y}_1 + \text{diag}\{\mathbf{1}^T Y_{11,22}\} & Y_{12,21} \\ Y_{12,21}^T & X_{22,11}^{-1} \end{bmatrix} := \begin{bmatrix} \hat{Y}_{11} & \hat{Y}_{12} \\ \hat{Y}_{12}^T & \hat{Y}_{22} \end{bmatrix}$   
 and set  $\bar{Y}_2 = X_{22,11}^{-1}$
  - 6: **if** the graph corresponding to  $\bar{Y}_2$ , i.e.,  $\mathcal{G}(\bar{Y}_2)$  is not radial **then**
  - 7:   **for** each pair of nodes  $(j, k)$  **do**
  - 8:     Compute  $\gamma[j, k]$  from  $\bar{Y}_2$ .
  - 9:   **end for**
  - 10: Solve for  $\text{diag}\{\mathbf{1}^T Y_{11,22}\}$ ,  $Y_{12,21}$  and  $X_{22,11}$  from (25)  
 and set  $\hat{Y} = \begin{bmatrix} \hat{Y}_{11} & \hat{Y}_{12} & 0 \\ \hat{Y}_{12}^T & \text{diag}\{\mathbf{1}^T Y_{11,22}\} & Y_{12,21} \\ 0 & Y_{12,21}^T & X_{22,11}^{-1} \end{bmatrix}$ .
  - 11: Set  

$$\hat{Y}_{11} = \begin{bmatrix} \hat{Y}_{11} & \hat{Y}_{12} \\ \hat{Y}_{12}^T & \text{diag}\{\mathbf{1}^T Y_{11,22}\} \end{bmatrix}, \hat{Y}_{12} = \begin{bmatrix} 0 \\ Y_{12,21} \end{bmatrix}.$$
  - 12: Set  $\bar{Y} = X_{22,11}^{-1}$  and apply Algorithm 2 to obtain  $\bar{Y}_1$  and  $\bar{Y}_2$ .
  - 13: **end if**
  - 14: **return**  $Y = \hat{Y}$
- 

<sup>3</sup>For notational simplicity, we assume without loss of generality that all measured nodes are boundary measured nodes. Yet, this assumption can easily be relaxed.

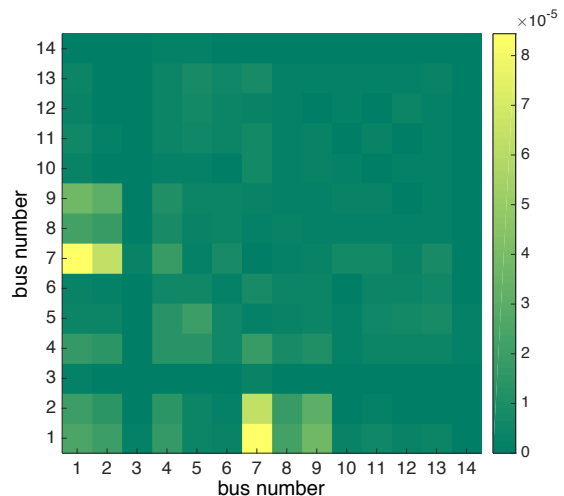


Fig. 4. The identification error when there is no hidden state. The color of a cell located at row  $i$  and column  $j$  represents the value of  $|Y[i, j] - \hat{Y}[i, j]|$ . It can be seen that the identification error using measurements of 15 time slots ( $K = 15$ ) is quite small compared to the absolute value of the elements of  $Y$ .

## V. SIMULATIONS

### A. Simulated data

In this section we implement the proposed algorithms in MATLAB and evaluate their identification accuracy by performing simulations in MATPOWER [22]. The optimization problems are solved using the CVX toolbox [23]. We run power flow analysis on the IEEE 14-bus test system, representing a portion of a power system in the Midwestern U.S., which has 14 buses, 11 aggregated loads, and 5 generators, 3 of which are synchronous compensators used for reactive power support [24]. To validate our identification algorithms in three-phase distribution systems, we have also performed simulations on IEEE test distribution networks, which are not presented here (see our previous work [25] for the identification results in distribution systems).

We assume that PMUs are installed at selected buses and that they can precisely measure the voltage and current magnitudes and phase angles that we obtain from power flow calculations, unless stated otherwise. For each scenario, we run 100 steady state simulations, each pertaining to a time slot, to determine the voltage and current magnitude and phase angle of every bus, while varying the real and reactive power demand of the loads across the time slots. Specifically, for a given time slot, the real and reactive power consumption of a constant PQ load are computed by multiplying a scaling factor drawn from a uniform distribution over the interval  $[0.8, 1.2]$  by the real and reactive power consumption data provided in [24]. We obtain the admittance matrix of this system using a built-in function of the power flow simulator. It turns out that the absolute values of nonzero complex elements of the admittance matrix are between 1.86 and 40.06, reminding the readers that a complex number's absolute value is its distance from zero in the complex plane.

We first consider the scenario that every bus is equipped with a PMU. Assuming that the self admittance of bus 7, i.e.,

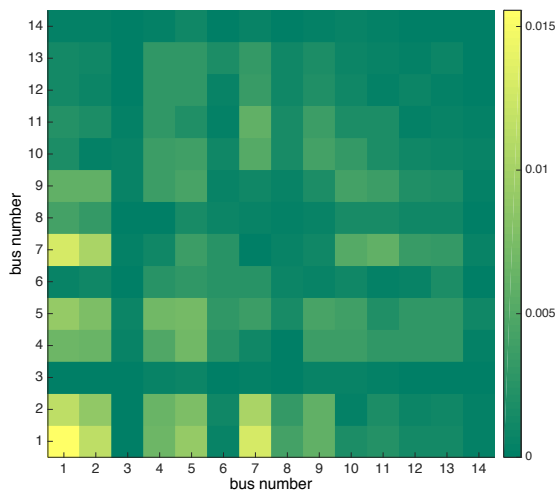


Fig. 5. The identification error when white Gaussian noise is added to both complex voltage and current measurements. Similar to the previous case, the errors are sufficiently small.

the transformer bus, is known, Fig. 4 shows the identification error, defined as  $|Y - \hat{Y}|$ , and the vertical color bar indicates the mapping of data values into colors. Hence, the color of a cell located at row  $i$  and column  $j$  represents the value of  $|Y[i, j] - \hat{Y}[i, j]|$ . It can be seen that the identification error using measurements of 15 time slots ( $K = 15$ ) is quite small compared to the absolute value of the elements of  $Y$ , and this error does not vary much if we use more observations. We next analyze the sensitivity of the proposed algorithm to the measurement error which is typically introduced by the transducers. To this end, white Gaussian noise with a signal-to-noise ratio of 125 is added to both complex voltage and current measurements. The signal-to-noise ratio is chosen such that the measurement accuracy lies within the reported range for existing PMU technology. Fig. 5 shows the absolute identification error for this case. Similar to the previous case, the errors are sufficiently small. In general, we observe that the identification error increases as we decrease the signal-to-noise ratio and it becomes really large when the signal-to-noise ratio drops below 100; at this point we say that the  $Y$  matrix cannot be identified from data.

### B. Experimental data

Next, we test the proposed IPF algorithm on the IEEE 5-bus benchmark shown in the left panel of Fig. 6. The network contains 4 dynamic loads, 2 generators and 7 transmission lines. The system admittance matrix is obtained from [26] with the absolute values of nonzero complex elements of the admittance matrix are between 3.80 and 31.32. Simulation is performed on OPAL-RT real time simulator [27] in our lab shown in the right panel of Fig. 6. The generator is represented by a sixth order model with turbine governors and excitation systems. Assume that the sampling frequency of PMU is 20 Hz and the dynamic loads change over time. We collect PMU data (nodal voltages and injected currents) of all buses for 40 seconds. Note that the frequency fluctuates with changes of the load demands, which is consistent with field measurements;

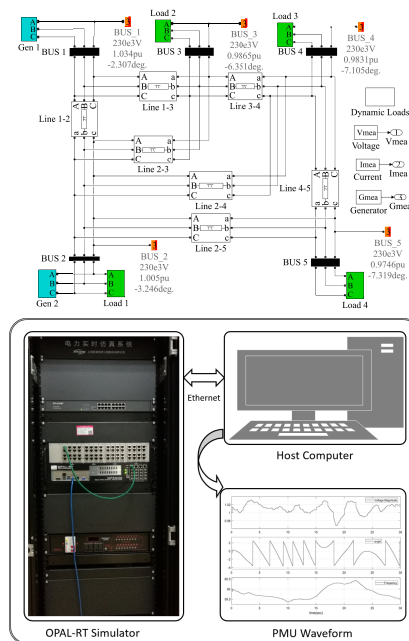


Fig. 6. Left: The network topology of the 5-bus benchmark systems. Right: The OPAL-RT real-time simulation platform that are used for data generation.

PMU has 0.49% average total vector error in simulation. Fig. 7 shows the identification error, defined as  $|Y - \hat{Y}|$  (element-wise absolute value), and the vertical color bar indicates the mapping of data values into colors. One can see that the IPF is capable of identifying the topology correctly and estimating system parameters with small error from noisy data with the maximum parameter estimation error 0.2126.

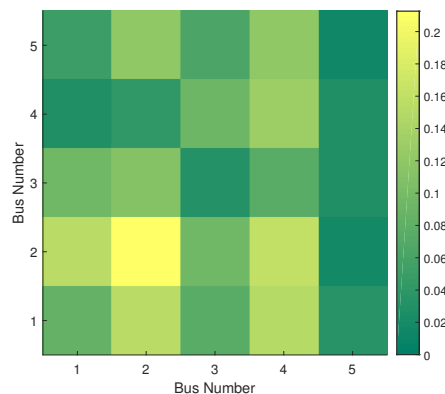


Fig. 7. The identified error of admittance matrix along buses for the 5-bus benchmark example we tried.

### C. Hidden node case

Given a graph shown in Fig. 8 (left), if sensors are deployed at nodes  $\mathcal{M} = \{1, 2, 6, 7, 8, 9, 12\}$ , we can use Kron reduction to obtain the graph shown in Fig. 8 (right). In this example, the hidden nodes are  $\mathcal{H} = \{3, 4, 5, 10, 11\}$ , from which nodes  $\{3, 5, 10, 11\}$  have degree less than 3, and therefore, cannot

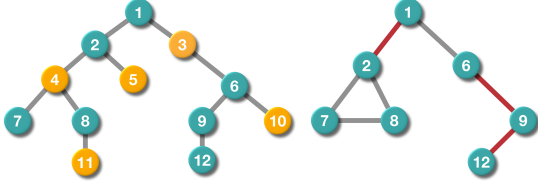


Fig. 8. An example of a 12-bus network. **Left:** The original network topology. Green circles denote the observed nodes while yellow ones denote the hidden nodes. **Right:** The topology of the condensed graph obtained from Kron reduction. The red lines denote the edges in  $\mathcal{G}_1$  and the grey ones denote the ones in  $\mathcal{G}_2$ .

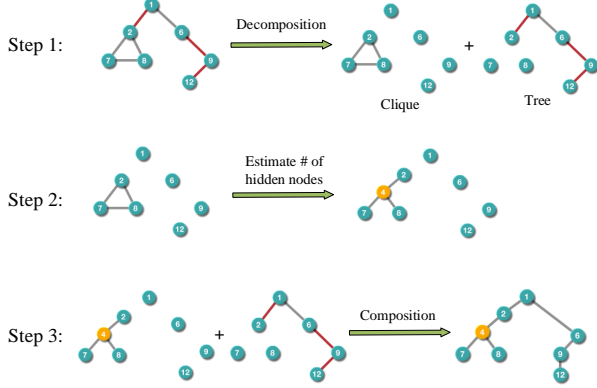


Fig. 9. A step-by-step illustration of the proposed algorithm. Step 1 is described in Algorithm 2 that one separates the graph to a number of cliques and a forest. Step 2 is described in Algorithm 3 that one recovers the admittance submatrix from every clique. Step 3 combines all the recovered graphs (together with admittance submatrices) to recover the whole admittance matrix.

be identified from data. We now illustrate how the proposed algorithm can identify the actual admittance matrix including Node 4.

The first step is to decompose the graph corresponding to the estimated  $\bar{Y}$  matrix to two graphs using Algorithm 2, one is a collection of cliques and the other one is a tree and some isolated nodes. The second step is to apply Algorithm 3 to identify the original admittance matrices for all cliques. The final step is to take the union of the cliques and the graph obtained in the second step. These steps are shown in Fig. 9.

Indeed, even the original graph does not satisfy the assumption on the degree of hidden nodes. We can recover a graph with smallest number of nodes that is a) consistent with  $\bar{Y}$  and b) satisfies Assumption 3.

Consider another graph with the following topology in Fig. 10, the admittance matrix has the following form<sup>4</sup>:

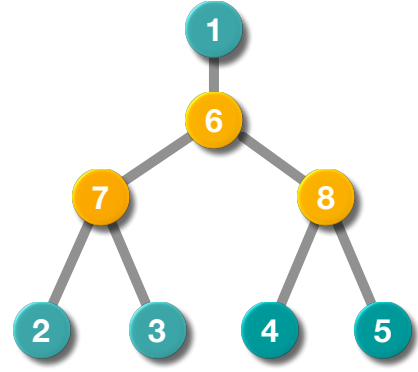


Fig. 10. An example of a 8-bus network, where 5 nodes are measured, and there exists three hidden nodes.

$$Y = \begin{bmatrix} Y_{11} & 0 & 0 & 0 & 0 & -Y_{16} & 0 & 0 \\ & Y_{22} & 0 & 0 & 0 & 0 & -Y_{27} & 0 \\ & & Y_{33} & 0 & 0 & 0 & -Y_{37} & 0 \\ & & & Y_{44} & 0 & 0 & 0 & -Y_{48} \\ & & & & Y_{55} & 0 & 0 & -Y_{58} \\ & & & & & Y_{66} & -Y_{67} & -Y_{68} \\ & & & & & & Y_{77} & 0 \\ & & & & & & & Y_{88} \end{bmatrix}.$$

Through direct computation, we have

$$\bar{Y} = \begin{bmatrix} Y_{11} - X_{11}Y_{16}^2 & -X_{12}Y_{16}Y_{27} & -X_{12}Y_{16}Y_{37} & -X_{13}Y_{16}Y_{48} & -X_{13}Y_{16}Y_{58} \\ & Y_{22} - X_{22}Y_{27}^2 & -X_{22}Y_{27}Y_{37} & -X_{23}Y_{27}Y_{48} & -X_{23}Y_{27}Y_{58} \\ & & Y_{33} - X_{22}Y_{37}^2 & -X_{22}Y_{37}Y_{48} & -X_{23}Y_{37}Y_{58} \\ & & & Y_{44} - X_{33}Y_{48}^2 & -X_{33}Y_{48}Y_{58} \\ & & & & Y_{55} - X_{33}Y_{58}^2 \end{bmatrix}.$$

For the ‘zero shunt element’ case, we follow Algorithm 3. For starters, we compute  $\gamma$

$$\gamma = \begin{bmatrix} * & 0 & 0 & 0 & 0 \\ & * & 1 & 0 & 0 \\ & & * & 0 & 0 \\ & & & * & 1 \\ & & & & * \end{bmatrix}.$$

It means that nodes 2 and 3 are connected to the same hidden node, and nodes 4 and 5 are connected to the same hidden node. Thus, it is straightforward to compute  $Y_{22}, Y_{33}, Y_{44}, Y_{55}, X_{22}, X_{23}, X_{33}$  from  $\bar{Y}$  and furthermore  $Y_{27} = -Y_{22}, Y_{37} = -Y_{33}, Y_{48} = -Y_{44}, Y_{58} = -Y_{55}$ . Next, we obtain a ‘new’  $\bar{Y}$  by including two new hidden boundary nodes as measured nodes in eq. (29), where  $[X_{12}Y_{16} \ X_{13}Y_{16}]$  can be computed from the corresponding row of  $\bar{Y}$  and

$$\bar{Y}_{\text{new},11} = Y_{11} - X_{11}Y_{16}^2 + [X_{12}Y_{16} \ X_{13}Y_{16}] \begin{bmatrix} X_{22} & X_{23} \\ X_{23} & X_{33} \end{bmatrix}^{-1} \begin{bmatrix} X_{12}Y_{16} \\ X_{13}Y_{16} \end{bmatrix}.$$

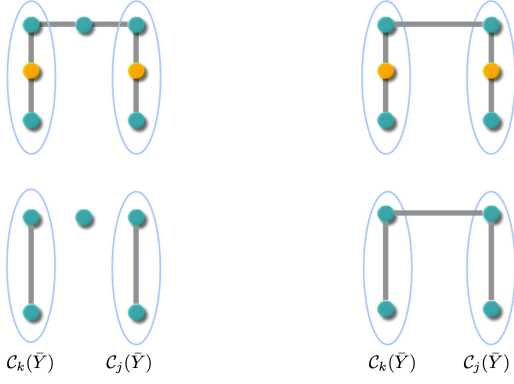
It is noted that nodes 2, 3, 4, 5 have no connections to non hidden boundary nodes, then they can be removed.

$$\bar{Y}_{\text{new}} = \begin{bmatrix} Y_{11} - Y_{66}^{-1}Y_{16}^2 & & & & \\ & Y_{77} & 0 & & \\ & 0 & Y_{88} & & \\ & & & -Y_{66}^{-1} \begin{bmatrix} Y_{67} \\ Y_{68} \end{bmatrix} & \\ & & & & \begin{bmatrix} Y_{67} \\ Y_{68} \end{bmatrix} \end{bmatrix}.$$

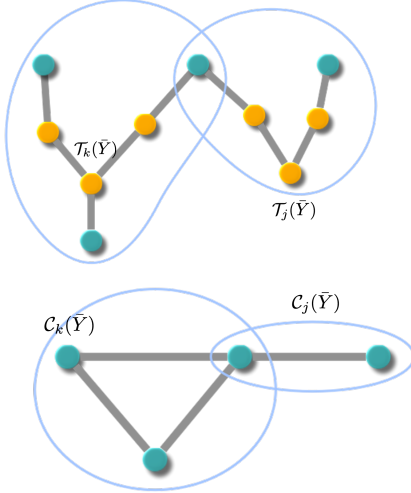
The last equality due to matrix inverse lemma. We can repeat

<sup>4</sup>For notational simplicity, we used  $Y_{ij}$  to denote the  $Y[i, j]$  element in this section.





(a) Disconnected maximal cliques (b) Connected by a line in  $Y_{11,22}$



(c) Connected by a boundary observed node

Fig. 11. Examples of maximal cliques in  $\bar{\mathcal{G}}_2$ . Shaded nodes are measured nodes and unshaded nodes are hidden nodes. (These examples do not satisfy Assumptions 3.2).

reductions  $\bar{Y}^j$  and  $\bar{Y}^k$  respectively are:

$$Y^j =: \left[ \begin{array}{c|cc} \hat{Y}_{11,22}^j & Y_{12,21}^j & 0 \\ \hline & Y_{22,11}^j & Y_{22,12}^j \\ & & Y_{22,22}^j \end{array} \right] \quad (32a)$$

$$Y^k =: \left[ \begin{array}{c|cc} \hat{Y}_{11,22}^k & Y_{12,21}^k & 0 \\ \hline & Y_{22,11}^k & Y_{22,12}^k \\ & & Y_{22,22}^k \end{array} \right]. \quad (32b)$$

Then the admittance matrix  $Y$  of the overall network is shown in (33), where the top-left submatrix  $Y_{11}$  of  $Y$  has the same structure as  $\bar{Y}$  in (30). The submatrices  $Y_{11,11}$  and  $Y_{11,12}$  correspond to the subgraph of *internal* measured nodes and their connectivity to boundary measured nodes. They can be identified directly from the given Kron-reduced admittance matrix  $\bar{Y}$  of the overall network. The submatrices  $\hat{Y}_{11,22}^j$  and  $\hat{Y}_{11,22}^k$  are obtain from  $Y_{11,22}^j$ ,  $Y_{11,22}^k$  and  $Y_{11,12}$  by modifying the diagonal entries of  $Y_{11,22}^j$  and  $Y_{11,22}^k$  respectively so that

$Y$  has zero row and column sums, i.e.,

$$\begin{bmatrix} \hat{Y}_{11,22}^j & 0 \\ 0 & \hat{Y}_{11,22}^k \end{bmatrix} := \begin{bmatrix} Y_{11,22}^j & 0 \\ 0 & Y_{11,22}^k \end{bmatrix} - \text{diag}(\mathbf{1}^T Y_{11,12}).$$

**Case 2: Figure 11(b).**  $C_j(\bar{Y})$  and  $C_k(\bar{Y})$  are connected by a line in  $Y_{11,22}$  between two boundary observed nodes. The Kron-reduced matrix  $\bar{Y}$  is of the form:

$$\bar{Y} = \begin{bmatrix} \times & \times & \times \\ \times & \times & \times \\ & \times & \times & \times \\ & & \times & \times & \times \\ & & & \times & \times \end{bmatrix} =: \begin{bmatrix} W_{11} & W_{12} \\ W_{12}^T & W_{22} \end{bmatrix} \quad (34)$$

where the submatrix  $W_{11}$  shaded in red corresponds to the maximal clique  $C_j(\bar{Y})$  and the submatrix  $W_{22}$  shaded in blue corresponds to  $C_k(\bar{Y})$ . The admittance matrices  $\bar{Y}^j$  and  $\bar{Y}^k$  of the maximal cliques  $C_j(\bar{Y})$  and  $C_k(\bar{Y})$  respectively are given by (31).

Suppose the admittance matrices  $Y^j$  and  $Y^k$  identified from their Kron-reduced matrices  $\bar{Y}^j$  and  $\bar{Y}^k$  respectively are given by (32). Then the admittance matrix  $Y$  of the overall network is

$$Y = \left[ \begin{array}{cc|cccc} \hat{Y}_{11,22}^j & W_{12} & Y_{12,21}^j & 0 & 0 & 0 \\ W_{12}^T & \hat{Y}_{11,22}^k & 0 & Y_{12,21}^k & 0 & 0 \\ \hline & & Y_{22,11}^j & 0 & Y_{22,12}^j & 0 \\ & & 0 & Y_{22,11}^k & 0 & Y_{22,12}^k \\ & & & & Y_{22,22}^j & 0 \\ & & & & & 0 & Y_{22,22}^k \end{array} \right]$$

$$=: \begin{bmatrix} Y_{11} & Y_{12} \\ Y_{12}^T & Y_{22} \end{bmatrix},$$

where the submatrix  $Y_{11}$  of  $Y$  has the same structure as  $\bar{Y}$  in (34). The submatrices  $\hat{Y}_{11,22}^j$  and  $\hat{Y}_{11,22}^k$  are obtain from  $Y_{11,22}^j$ ,  $Y_{11,22}^k$  and  $W_{12}$  by modifying the diagonal entries of  $Y_{11,22}^j$  and  $Y_{11,22}^k$  respectively so that  $Y$  has zero row and column sums, i.e.,

$$\hat{Y}_{11,22}^j := Y_{11,22}^j - \text{diag}(W_{12}\mathbf{1})$$

$$\hat{Y}_{11,22}^k := Y_{11,22}^k - \text{diag}(\mathbf{1}^T W_{12}).$$

**Case 3: Figure 11(c).**  $C_j(\bar{Y})$  and  $C_k(\bar{Y})$  are connected by a shared boundary observed node. The Kron-reduced matrix  $\bar{Y}$  is of the form:

$$\bar{Y} = \begin{bmatrix} \times & \times & \times \\ \times & \times & \times \\ \times & \times & \times \\ & \times & \times & \times \\ & & \times & \times \end{bmatrix} \quad (35)$$

where the submatrix  $W_{11}$  shaded in red corresponds to the maximal clique  $C_j(\bar{Y})$  and the submatrix  $W_{22}$  shaded in blue corresponds to  $C_k(\bar{Y})$ . The admittance matrices  $\bar{Y}^j$  and  $\bar{Y}^k$  of the maximal cliques  $C_j(\bar{Y})$  and  $C_k(\bar{Y})$  respectively are given by (31).

The two maximal cliques  $C_j(\bar{Y})$  and  $C_k(\bar{Y})$  are connected by a single shared node. Suppose without loss of generality that the last row/column of  $\bar{Y}^j$  and the first row/column of



$$Y = \left[ \begin{array}{cc|cccc} Y_{11,11} & Y_{11,12} & 0 & 0 & 0 & 0 \\ \hline & \hat{Y}_{11,22}^j & 0 & & & \\ & 0 & \hat{Y}_{11,22}^k & & & \\ \hline & & & Y_{12,21}^j & 0 & 0 & 0 \\ & & & 0 & Y_{12,21}^k & 0 & 0 \\ \hline & & & Y_{22,11}^j & 0 & Y_{22,12}^j & 0 \\ & & & 0 & Y_{22,11}^k & 0 & Y_{22,12}^k \\ & & & & & Y_{22,22}^j & 0 \\ & & & & & 0 & Y_{22,22}^k \\ & & & & & 0 & Y_{22,22}^k \end{array} \right] =: \begin{bmatrix} Y_{11} & Y_{12} \\ Y_{12}^T & Y_{22} \end{bmatrix}. \quad (33)$$

$\bar{Y}^k$  correspond to the shared node. Suppose the admittance matrices  $Y^j$  and  $Y^k$  identified from  $\bar{Y}^j$  and  $\bar{Y}^k$  respectively are

$$Y^j =: \left[ \begin{array}{cc|cc} \hat{Y}_{11,22}^j & \hat{r}_{11,22}^{jT} & Y_{12,21}^j & 0 \\ \hat{r}_{11,22}^j & d_{11,22}^j & r_{12,21}^j & 0 \\ \hline & & Y_{22,11}^j & Y_{22,12}^j \\ & & & Y_{22,22}^j \end{array} \right]$$

$$Y^k =: \left[ \begin{array}{cc|cc} d_{11,22}^k & \hat{r}_{11,22}^k & r_{12,21}^k & 0 \\ \hat{r}_{11,22}^{kT} & \hat{Y}_{11,22}^k & Y_{12,21}^k & 0 \\ \hline & & Y_{22,11}^k & Y_{22,12}^k \\ & & & Y_{22,22}^k \end{array} \right],$$

where  $(\hat{r}_{11,22}^j, d_{11,22}^j, r_{12,21}^j)$  and  $(\hat{r}_{11,22}^k, d_{11,22}^k, r_{12,21}^k)$  are the rows corresponding to the shared node. For the example in Figure 11(c),  $\hat{Y}_{11,22}^j$  is  $2 \times 2$  and  $\hat{r}_{11,22}^j$  is  $1 \times 2$ ; both  $\hat{Y}_{11,22}^k$  and  $\hat{r}_{11,22}^k$  are  $1 \times 1$ .

To construct the admittance matrix  $Y$  of the overall network, the rows in  $Y^j$  and  $Y^k$  corresponding to this shared node is combined into a single row:

$$\left[ \hat{r}_{11,22}^j \quad d_{11,22}^j + d_{11,22}^k \quad \hat{r}_{11,22}^k \mid r_{12,21}^j \quad r_{12,21}^k \right]$$

The admittance matrix  $Y$  is then

$$Y = \left[ \begin{array}{cc|cccc} \hat{Y}_{11,22}^j & \hat{r}_{11,22}^{jT} & 0 & Y_{12,21}^j & 0 & 0 & 0 \\ \hat{r}_{11,22}^j & d_{11,22}^j + d_{11,22}^k & \hat{r}_{11,22}^k & r_{12,21}^j & r_{12,21}^k & 0 & 0 \\ 0 & \hat{r}_{11,22}^{kT} & \hat{Y}_{11,22}^k & 0 & Y_{12,21}^k & 0 & 0 \\ \hline & & & Y_{22,11}^j & 0 & Y_{22,12}^j & 0 \\ & & & 0 & Y_{22,11}^k & 0 & Y_{22,12}^k \\ & & & & & Y_{22,22}^j & 0 \\ & & & & & 0 & Y_{22,22}^k \end{array} \right] =: \begin{bmatrix} Y_{11} & Y_{12} \\ Y_{12}^T & Y_{22} \end{bmatrix},$$

where submatrix  $Y_{11}$  of  $Y$  has the same structure as  $\bar{Y}$  in (35).

## REFERENCES

- [1] K. Dehghanpour, Z. Wang, J. Wang, Y. Yuan, and F. Bu, "A survey on state estimation techniques and challenges in smart distribution systems," *IEEE Transactions on Smart Grid*, vol. 10, no. 2, pp. 2312–2322, 2018.
- [2] C. Le Floch, S. Bansal, C. J. Tomlin, S. J. Moura, and M. N. Zeilinger, "Plug-and-play model predictive control for load shaping and voltage control in smart grids," *IEEE Transactions on Smart Grid*, vol. 10, no. 3, pp. 2334–2344, 2017.
- [3] O. Ardakanian, V. W. Wong, R. Dobbe, S. H. Low, A. von Meier, C. J. Tomlin, and Y. Yuan, "On identification of distribution grids," *IEEE Transactions on Control of Network Systems*, vol. 6, no. 3, pp. 950–960, 2019.
- [4] P. Zhuang, R. Deng, and H. Liang, "False data injection attacks against state estimation in multiphase and unbalanced smart distribution systems," *IEEE Transactions on Smart Grid*, vol. 10, no. 6, pp. 6000–6013, 2019.
- [5] F. Dorfler and F. Bullo, "Kron Reduction of Graphs With Applications to Electrical Networks," *IEEE Transactions on Circuits and Systems I: Regular Papers*, vol. 60, no. 1, pp. 150–163, Jan 2013.
- [6] X. Li, H. V. Poor, and A. Scaglione, "Blind topology identification for power systems," in *Proc. IEEE SmartGridComm*, 2013.
- [7] V. Kekatos, G. B. Giannakis, and R. Baldick, "Grid topology identification using electricity prices," in *IEEE PES General Meeting — Conference Exposition*, July 2014, pp. 1–5.
- [8] M. Babakmehr, M. G. Simoes, M. B. Wakin, and F. Harirchi, "Compressive Sensing-Based Topology Identification for Smart Grids," *IEEE Transactions on Industrial Informatics*, vol. 12, no. 2, pp. 532–543, April 2016.
- [9] Y. Yuan, X. Tang, W. Zhou, W. Pan, X. Li, H.-T. Zhang, H. Ding, and J. Goncalves, "Data driven discovery of cyber physical systems," *Nature communications*, vol. 10, no. 1, pp. 1–9, 2019.
- [10] D. Deka, S. Backhaus, and M. Chertkov, "Estimating distribution grid topologies: A graphical learning based approach," in *2016 Power Systems Computation Conference (PSCC)*, 2016, pp. 1–7.
- [11] Y. Liao, Y. Weng, M. Wu, and R. Rajagopal, "Distribution grid topology reconstruction: An information theoretic approach," in *North American Power Symposium*, Oct 2015, pp. 1–6.
- [12] Y. Liao, Y. Weng, and R. Rajagopal, "Urban Distribution Grid Topology Reconstruction via Lasso," in *IEEE PES General Meeting*, July 2016, pp. 1–6.
- [13] J. Yu, Y. Weng, and R. Rajagopal, "Patopa: A data-driven parameter and topology joint estimation framework in distribution grids," *IEEE Transactions on Power Systems*, vol. 33, no. 4, pp. 4335–4347, 2017.
- [14] S. Park, D. Deka, S. Backhaus, and M. Chertkov, "Learning with end-users in distribution grids: Topology and parameter estimation," *IEEE Transactions on Control of Network Systems*, vol. 7, no. 3, pp. 1428–1440, 2020.
- [15] H. Zhu and G. B. Giannakis, "Sparse overcomplete representations for efficient identification of power line outages," *IEEE Transactions on Power Systems*, vol. 27, no. 4, pp. 2215–2224, November 2012.
- [16] D. Deka, S. Backhaus, and M. Chertkov, "Structure learning in power distribution networks," *IEEE Transactions on Control of Network Systems*, vol. 5, no. 3, pp. 1061–1074, September 2018.
- [17] G. Cavraro and V. Kekatos, "Graph algorithms for topology identification using power grid probing," *IEEE control systems letters*, vol. 2, no. 4, pp. 689–694, 2018.
- [18] G. Cavraro, V. Kekatos, and S. Veeramachaneni, "Voltage analytics for power distribution network topology verification," *IEEE Transactions on*

*Smart Grid*, vol. 10, no. 1, pp. 1058–1067, 2017.

- [19] H. Li, Y. Weng, Y. Liao, B. Keel, and K. E. Brown, “Distribution grid impedance & topology estimation with limited or no micro-pmus,” *International Journal of Electrical Power & Energy Systems*, vol. 129, p. 106794, 2021.
- [20] S. Wright and J. Nocedal, “Numerical optimization,” *Springer Science*, vol. 35, pp. 67–68, 1999.
- [21] Y. Yuan, O. Ardakanian, S. Low, and C. Tomlin, “On the inverse power flow problem,” *arXiv preprint arXiv:1610.06631*, 2016.
- [22] R. D. Zimmerman, C. E. Murillo-Sanchez, and R. J. Thomas, “MATPOWER: Steady-State Operations, Planning, and Analysis Tools for Power Systems Research and Education,” *IEEE Transactions on Power Systems*, vol. 26, no. 1, pp. 12–19, Feb 2011.
- [23] M. Grant and S. Boyd, “CVX: Matlab software for disciplined convex programming, version 2.1,” <http://cvxr.com/cvx>, Mar. 2014.
- [24] IEEE, “14 Bus Test Case,” [https://www.ee.washington.edu/research/pstca/pf14/pg\\_tca14bus.htm](https://www.ee.washington.edu/research/pstca/pf14/pg_tca14bus.htm).
- [25] O. Ardakanian, Y. Yuan, R. Dobbe, A. von Meier, S. Low, and C. Tomlin, “Event detection and localization in distribution grids with phasor measurement units,” in *IEEE Power Energy Society General Meeting*, July 2017, pp. 1–5.
- [26] “IEEE 5 bus test system data,” [http://shodhganga.inflibnet.ac.in/bitstream/10603/26549/14/14\\_appendix.pdf](http://shodhganga.inflibnet.ac.in/bitstream/10603/26549/14/14_appendix.pdf), [Online; accessed 20-Jan-2019].
- [27] “OPAL-RT real-time digital simulator,” <https://www.opal-rt.com/simulator-platform-op5600/>, [Online; accessed 20-Jan-2019].



**Omid Ardakanian** (M’15) is an Assistant Professor at the University of Alberta, Canada. He received his B.Sc. from Sharif University of Technology in 2009, and M.Math. and Ph.D. from the University of Waterloo in 2011 and 2015. From 2015 to 2017, he was an NSERC Postdoctoral Fellow at UC Berkeley and the University of British Columbia. He received best paper awards at ACM e-Energy, ACM BuildSys, and IEEE PES General Meeting. His research focuses on the design and implementation of intelligent networked systems.



**Ye Yuan** (M’13, SM’20) received the B.Eng. degree from the Department of Automation, Shanghai Jiao Tong University, Shanghai, China, in 2008, and the M.Phil. and Ph.D. degrees from the Department of Engineering, University of Cambridge, Cambridge, U.K., in 2009 and 2012, respectively. He has been a Full Professor at the Huazhong University of Science and Technology, Wuhan, China since 2016. Prior to that, he was a Postdoctoral Researcher at UC Berkeley, a Junior Research Fellow at Darwin College, University of Cambridge. His research interests

include system identification and optimization with applications to cyber-physical systems.



**Claire J. Tomlin** (F’10) is the Charles A. Desoer Professor of Engineering in the Department of Electrical Engineering and Computer Sciences (EECS), University of California Berkeley (UC Berkeley). She was an Assistant, Associate, and Full Professor in Aeronautics and Astronautics at Stanford University from 1998 to 2007, and in 2005, she joined UC Berkeley. Claire works in the area of control theory and hybrid systems, with applications to air traffic management, UAV systems, energy, robotics, and systems biology. She is a MacArthur Foundation

Fellow (2006), an IEEE Fellow (2010), and in 2017, she was awarded the IEEE Transportation Technologies Award. In 2019, Claire was elected to the National Academy of Engineering and the American Academy of Arts and Sciences.



**Steven Low** (F’08) is the F. J. Gilloon Professor of the Department of Computing & Mathematical Sciences and the Department of Electrical Engineering at Caltech and an Honorary Professor of the University of Melbourne. Before that, he was with AT&T Bell Laboratories, Murray Hill, NJ, and the University of Melbourne, Australia. He has held honorary/chaired professorship in Australia, China and Taiwan. He was a co-recipient of IEEE best paper awards, an awardee of the IEEE INFOCOM Achievement Award and the ACM SIGMETRICS

Test of Time Award, and is a Fellow of IEEE, ACM, and CSEE. He was well-known for work on Internet congestion control and semidefinite relaxation of optimal power flow problems in smart grid. His research on networks has been accelerating more than 1TB of Internet traffic every second since 2014. His research on smart grid is providing large-scale cost effective electric vehicle charging to workplaces. He received his B.S. from Cornell and PhD from Berkeley, both in EE.